

Combined exercise intervention in a mouse model of high-risk neuroblastoma: effects on physical, immune, tumor and clinical outcomes.

Cecilia Rincón-Castanedo¹, Asunción Martín-Ruiz^{1,2*}, Sandra Zazo^{3*}, Ana L. Luis Huertas⁴, Pedro L. Valenzuela^{5,6}, María Morán^{7,8}, Steven J. Fleck¹, Alejandro Santos-Lozano^{5,9}, Manuel Ramírez^{10,11,12}, Federico Rojo³, Alejandro Lucia^{1,5**}, África González-Murillo^{10,11,12**}, Carmen Fiuza-Luces^{5**}

*These two authors share the same position

**Share senior authorship

¹ Faculty of Sport Sciences, Universidad Europea de Madrid, Madrid, Spain

² Biophysics & Systems Biology Group. Department of Biochemistry and Molecular Biology, Complutense University of Madrid (UCM). Madrid, Spain

³ Pathology, Fundación Jiménez Díaz University, Hospital Health Research Institute (IIS—FJD, UAM)—CIBERONC, Madrid, Spain

⁴ Servicio de Cirugía Pediátrica, Hospital Infantil Universitario Niño Jesús, Madrid, Spain

⁵ Physical Activity and Health Research Group ('PAHERG'), Instituto de Investigación Sanitaria Hospital '12 de Octubre' ('imas12'), Madrid, Spain

⁶ Department of Systems Biology, University of Alcalá, Alcalá de Henares, Spain

⁷ Mitochondrial and Neuromuscular Diseases Laboratory, Instituto de Investigación Sanitaria Hospital '12 de Octubre' ('imas12'), Madrid, Spain

⁸ Spanish Network for Biomedical Research in Rare Diseases (CIBERER), U723, Madrid, Spain

⁹ i+HeALTH, Department of Health Sciences, European University Miguel de Cervantes, Valladolid, Spain

¹⁰ Unidad de Terapias Avanzadas, Oncología, Hospital Infantil Universitario Niño Jesús, Madrid, Spain

¹¹ Fundación de Investigación Biomédica, Hospital Infantil Universitario Niño Jesús, Madrid, Spain

¹² Instituto de Investigación Sanitaria La Princesa, Madrid, Spain

ABSTRACT

Background: Exercise might exert anti-tumoral effects in adult cancers but this question remains open in pediatric tumors, which frequently show a different biology compared to adult malignancies. We studied the effects of an exercise intervention on physical function, immune variables and tumoral response in a preclinical model of a highly aggressive pediatric cancer, high-risk neuroblastoma (HR-NB).

Methods: 6-8-week-old male mice with orthotopically-induced HR-NB were assigned to a control (N=13) or exercise (5-week combined [aerobic+resistance]) group (N=17). Outcomes included physical function (cardiorespiratory fitness [CRF] and muscle strength), as well as related muscle molecular indicators, blood and tumor immune cell and molecular variables, tumor progression, clinical severity, and survival.

Results: Exercise attenuated CRF decline (p=0.029 for the

group-by-time interaction effect), which was accompanied by higher muscle levels of oxidative capacity (citrate synthase and respiratory chain complexes III, IV and V) and an indicator of antioxidant defense (glutathione reductase) in the intervention arm (all p≤0.001), as well as by higher levels of apoptosis (caspase-3, p=0.029) and angiogenesis (vascular endothelial growth factor receptor-2, p=0.012). The proportion of 'hot-like' (i.e., with viable immune infiltrates in flow cytometry analyses) tumors tended to be higher (p=0.0789) in the exercise group (76.9%, vs. 33.3% in control mice). Exercise also promoted greater total immune (p=0.045) and myeloid cell (p=0.049) infiltration within the 'hot' tumors, with a higher proportion of two myeloid cell subsets (CD11C+ [dendritic] cells [p=0.049] and M2-like tumor-associated macrophages [p=0.028]), yet with no significant changes in lymphoid infiltrates or in circulating immune cells or chemokines/cytokines. No training effect was found either for muscle strength or anabolic status, cancer progression (tumor weight and metastasis, tumor microenvironment), clinical severity, or survival.

Conclusions: Combined exercise appears as an effective strategy for attenuating physical function decline in a mouse model of HR-NB, also exerting some potential immune benefits within the tumor, which seem overall different from those previously reported in adult cancers.

Key words: cancer; pediatric cancer; exercise; immune function; immuno-oncology

*Correspondence to:

Carmen Fiuza-Luces, PhD

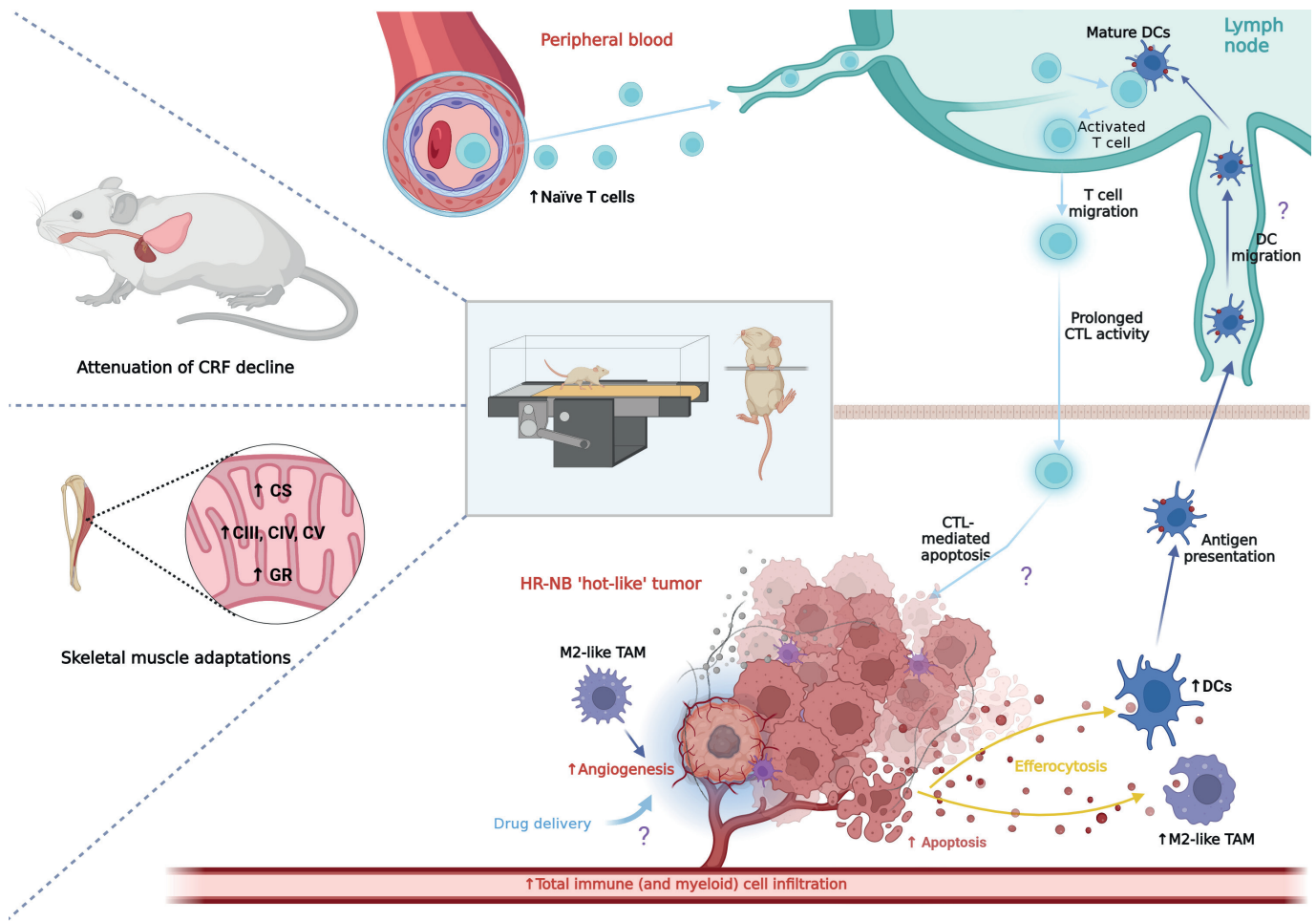
Physical Activity and Health Research Group (PAHERG)

Instituto de Investigación Sanitaria Hospital Universitario 12 de Octubre ('imas12')

Centro de Actividades Ambulatorias (CAA), 7ª Planta, Bloque D

Av. de Córdoba s/n, 28041 Madrid, Spain

Phone: +34 91 779 2713; e-mail: cfuza.imas12@h12o.es



Graphical abstract: Main effects of the exercise intervention and proposed potential mechanisms*. Abbreviations: CRF, cardiorespiratory fitness; CS, citrate synthase; CIII, CIV and CV, mitochondrial respiratory complex III, IV and V, respectively; CTL, cytotoxic T lymphocytes; DC, dendritic cells; HR-NB, high-risk neuroblastoma; TAM, tumor associated macrophages. * Naïve T cells (which were found in higher proportions in the blood of the exercise group than in control mice) constantly circulate through secondary lymphoid organs, where antigen encounter occurs. For a CTL response, antigen is brought to the lymph node via the lymphatic system by antigen presenting cells (which are typically DCs that mature after antigen acquisition in nonlymphoid tissues and migrate to the lymph node).

INTRODUCTION

A healthy lifestyle that includes regular physical activity is associated not only with a lower incidence of different types of adult cancers [1–4], but also with a lower risk of tumor recurrence or cancer-specific mortality [5–8]. Although most research has focused on the benefits of ‘aerobic’ physical activity (e.g., brisk walking, jogging), growing evidence also suggests that muscle resistance (or ‘strength’) exercise training – which together with aerobic activities is recommended by the World Health Organization (WHO) for health promotion in essentially all population groups [9] – can be associated with a lower risk of cancer and cancer-specific mortality [10]. In turn, epidemiological evidence is supported by preclinical research showing that regular aerobic exercise – typically voluntary (wheel) or forced (treadmill) running – could reduce tumor progression in rodents [11]. Although the different mechanisms underlying potential exercise antitumoral effects remain to be elucidated, an improvement in cancer immunosurveillance can be involved [12,13]. This is an important issue because the ability to evade immune destruction is one of the hallmarks of cancer [14], and immunotherapy (by means of stimulating natural immune defenses, e.g., using immunomodulators, monoclonal

antibodies, oncolytic viruses or checkpoint inhibitors) is gaining importance in oncology [13]. On the other hand, an active lifestyle is also able to attenuate the side effects of cancer and its treatment, notably fatigue and decreased physical function [15]. Thus, exercise has been reported to improve cardiorespiratory fitness (CRF) and overall physical function in cancer survivors, thereby contributing to a better health-related quality of life (HRQoL) [16].

Most research in the field of exercise and cancer – especially preclinical studies – has focused on adult malignancies, with comparatively less research conducted in pediatric cancer. In this effect, toxicities associated to pediatric cancer treatment (chemotherapy/radiotherapy) are often persistent years after treatment and include among others harmful changes to growth, impaired cardiopulmonary function (e.g., cardiotoxicity) and alterations in body composition (excess abdominal adiposity, muscle weakness, poor bone health), together with low physical performance and difficulty of coping with activities of daily living, as well as cognitive decline (with subsequent impairment in academic, social, and professional performance later in life) [17] whereas physical exercise interventions can have the opposite effect. There is indeed meta-analytical evidence that, especially when supervised, exercise interventions during and/

or after pediatric cancer treatment are safe and can increase or preserve physical capacity (e.g., CRF) [18], cardiac function [18], functional mobility during daily life activities [19], muscle strength [20], physical activity levels [20], body mass index [20] and cognitive function [21], while reducing fatigue [20]. In fact, Pediatric Oncology Exercise Guidelines have been recently developed to promote physical activity among children and adolescents affected by cancer [22]. However, whether physical exercise can also impact pediatric tumor development is unknown, except for a preclinical study on tumor vascular modulation in the context of Ewing sarcoma (a pediatric bone and soft tissue cancer) [23]. In this effect, the biology of children's tumors might considerably differ from that of adult malignancies, as the former are overall characterized by a distinct (and usually lower) mutational burden, an embryonal (or very early) origin in many cases and/or a dysregulation of developmental pathways, together with a lower contribution of environmental factors [24]. In addition, pediatric tumor development might often take place in a moment of life when the immune system is not yet totally developed [25], which does not usually occur until age ~7-8 years [26].

The two main types of pediatric tumors are leukemias (30%) and solid tumors, with neuroblastoma (NB) representing the commonest extracranial solid malignancy [27] – accounting for >7% of all pediatric cancers [28,29] and 15% of related deaths [29–31]. Most NB cases are diagnosed between 0 and 4 years of age (median age ~19 months) [32], with less than 5% of affected children older than 10 years [28]. On the other hand, more than half of patients are above the age threshold – see below – for a worse prognosis [32]. The biological and clinical heterogeneity of NB fluctuates from spontaneous regression to metastatic dissemination depending on factors such as age at diagnosis (with age >15 months associated with worse outcomes [33]), tumor size and localization, histopathological classification, genetic abnormalities, and status of the *MYCN* proto-oncogene [34,35]. In this effect, high-risk (HR)-NB is typically associated with older age at diagnosis, unfavorable histology, metastatic phenotypes, as well as with some genetic modifications (DNA ploidy or specific segmental chromosomal aberrations) and *MYCN* gene amplification, with the prognosis for affected children being one of the poorest in pediatric cancer (i.e., 5-year survival <40-50% and <10% in patients with relapsed and refractory disease, respectively) [33,36,37]. Whether exercise could exert a certain antitumoral effect in the context of such an aggressive tumor as HR-NB, or at least attenuate the decline in physical function commonly observed in these patients [38], is an important clinical question. In this context, the use of animal models could help to provide valuable insights.

The purpose of this study was to analyze the effects of a combined (aerobic and resistance) exercise intervention on physical function, clinical evolution, immune (blood and tumor) variables, and tumor microenvironment in a preclinical mouse model of HR-NB. Our hypothesis is that exercise could induce some potential benefits, particularly at the intratumoral immune level.

METHODS

Mice

The study was approved by the Ethics Committee on Animal Experimentation and Welfare of the Centro de Investigaciones

Energéticas, Medioambientales y Tecnológicas (CIEMAT; reference # ES280790000183, Madrid, Spain) and the Madrid Regional Department of Environment (reference # PROEX 036.7/21). All the study procedures were conducted in accordance with Animal Research: Reporting of In Vivo Experiments (ARRIVE) guidelines, as well as with the European (2010/63/UE Directive and European convention ETS 123) and Spanish (Law 6/2013 and Royal Decree 53/2013) regulations on animal protection in scientific research.

Wild-type 129/SvJ 6–8-week-old male mice were purchased from Vivotecnica (National Cancer Institute; Frederick, MD). They were bred and housed in the animal facility of CIEMAT under controlled conditions of temperature (20±2°C) and humidity (55±10%) with adequate environmental enrichment (nestlets), ventilation and constant 12-hour light/dark cycles, and with food and water provided ad libitum. They were used to generate an orthotopic murine model of HR-NB, as described below. All efforts were made to minimize animal suffering, which implied minimizing blood sampling and allowing a 3-week recovery period from surgery until baseline assessments.

Tumors

Cell cultures and preparation of neuroblastoma sphere-forming cells

The 36769-cell line kindly donated by Prof. Chesler (Royal Marsden NHS Foundation Trust; London, UK) was derived from a tumor mass developed in a TH-*MYCN*-129X1/SvJ transgenic mouse, which is a spontaneous model with *MYCN* amplification that recapitulates the genetic, histopathological, and clinical features of HR-NB [39]. These cells were maintained as described in previous research [40], using Dulbecco's Modified Eagle Medium/Nutrient Mixture F-12 (DMEM/F12) (Gibco; Carlsbad, CA) supplemented with 1% penicillin/streptomycin (Gibco), 1x B-27 without vitamin A (Gibco), 20 ng/mL murine epidermal growth factor (R&D Systems; Minneapolis, MN) and 40 ng/mL murine fibroblast growth factor (R&D Systems) at 37°C with 5% CO₂. The culture medium was renewed every 72 hours, and spheres were seed and expanded at 1/6 of initial concentration (for 8-10 days) before implantation. In the log phase of growth, they were transferred from the culture flask to a Falcon® tube and centrifuged at 900 g for 5 minutes. The spheres were incubated in trypsin (TripLE Express, Life Technologies; Carlsbad, CA) for 3-5 minutes at 37°C. Thereafter, the spheres were carefully mechanically-dissociated into single cells by pipetting, culture medium was added, the solution was centrifuged (1500 rpm, 5 minutes) and finally the cells were counted and prepared for later inoculation.

Implantation in mice

A single suspension of 1·10⁵ cells in 30 µL of unsupplemented DMEM/F12 was orthotopically inoculated into the left adrenal gland (which is where 40% of human NB tumors arise [41]) of the mice. This was done with an intraperitoneal approach through supraumbilical transverse laparotomy under general anesthesia – induced by an intraperitoneal injection of ketamine and dexmedetomidine (50 ng/g), using atipamezole (2.5 ng/g) as an anesthesia reversal agent.

Study design

During the 3-week period following surgery, the clinical

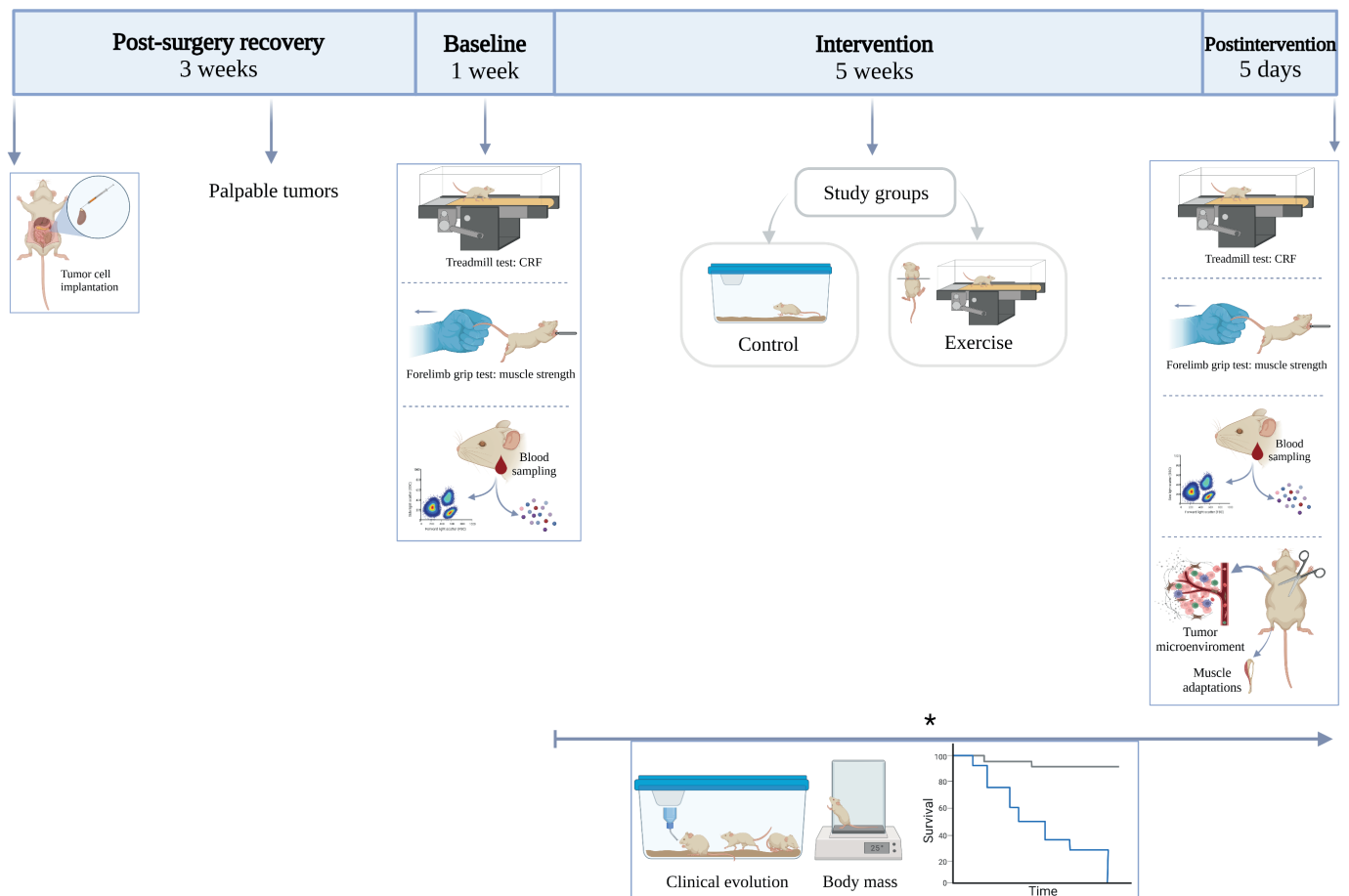


Figure 1. Study design. * Clinical evolution, body mass and survival (Kaplan Meyer curve) were determined from the start of the exercise intervention until death or end of the study (i.e., end of the 5-day postintervention phase).

evolution of the disease was evaluated every 2 days (Figure 1). Thus, mice were weighed and their posture, spontaneous activity, hair and scar were controlled to ascertain they had recovered from surgery. The post-surgery recovery phase was followed by the familiarization phase.

Familiarization

Mice were familiarized with the apparatuses and types of exercise involved in the physical evaluation tests – treadmill running (Harvard Apparatus, Panlab; Barcelona, Spain) and isometric force testing (Harvard Apparatus) [42]. This allowed the animals to gradually adapt to the new environmental conditions, and thus to reduce their stress levels while minimizing measurement error during physical testing. It also allowed us to ensure that the wound healing process had ended so that animals would be able to do the familiarization exercises (see below) and subsequent baseline physical tests safely.

The familiarization with the treadmill was performed on 3 separate days, by applying a gradual increase in running time, as well as in treadmill velocity and inclination (starting with 5 minutes at 5 cm/s and 5% inclination on the first day, and ending with a 12-minute run at 10 cm/s and 15% inclination on the third day, in all cases with an electrical stimulation of 0.1 mA). A total of 5 individual treadmills were used but each mouse was solely trained and tested with the same apparatus. Mice were also familiarized with the isometric force test, simulating the forelimb grip strength test on 3 separate days (see below).

Timing of physical tests and tissue/blood sampling

All the mice underwent the same physical tests (for determination of CRF and forelimb muscle strength) before (baseline) and after the intervention period. Blood sampling from the submandibular vein (200 μ L) was also performed at baseline (24 hours before the first battery of physical tests) and postintervention (48 hours after the last training session). Peripheral blood was drawn into EDTA or serum separator tubes (BD Microtainer®, Becton Dickinson; Franklin Lakes, NJ) in order to preserve the sample for immunophenotype analysis or to obtain (after centrifugation [1600 rpm, 5 minutes, twice]) a serum sample for analysis of cytokines/chemokines.

Mice were sacrificed by cervical dislocation after postintervention blood sampling and their tumors were excised, weighed and measured in 2 perpendicular dimensions using a vernier caliper for tumor volume calculations, and then divided into 3 pieces. One piece was fixed in 4% paraformaldehyde and embedded in paraffin prior to immunohistochemical studies. Another one was preserved in Hank's Balanced Salt Solution 1X (HBSS9) (Gibco) and appropriately mechanically-processed and enzymatically digested in RPMI 1640 medium with 1 mg/mL of collagenase D (Roche Diagnostics Corporation; Indianapolis, IN) to detect intratumoral immune cell infiltrates by flow cytometry. A third piece was frozen in liquid nitrogen and conserved at -80°C until gene expression analysis using real-time quantitative polymerase chain reaction (qRT-PCR). In addition, several tissues (kidneys, liver, gut, pancreas, spleen,

lung, brain) were extracted and fixed in formalin, excised and embedded in paraffin for hematoxylin and eosin (H&E) staining to detect potential metastasis. Finally, skeletal muscle tissue (tibialis anterior) was dissected, immediately frozen in liquid nitrogen and stored at -80°C until molecular analysis of muscle adaptations (see further below) by western blotting.

Group assignment

Mice were pair-matched based on the results of the treadmill tests. Thus, each two mice showing the closest values of CRF were matched together and randomly assigned to either an exercise or non-exercise (control) group. The former group performed the exercise training intervention that is described below whereas mice in the control group were allowed to freely move in the cage but only walked on the treadmill for 5 minutes (speed = 5 cm/s, inclination = 0%) once a week.

Intervention

The exercise intervention was designed following our previous experience with other mouse models [42,43], with slight modifications based on the singularities of the HR-NB model used in the present study. The program (4 days/week [Monday to Thursday], 40-60 minutes per day) lasted 5 weeks in total.

Aerobic training

All the sessions were performed between 09.00 am and 13.00 pm and included an aerobic (treadmill) training component, starting and ending with a warm-up and cool-down period, respectively (5-8 minutes at 35-40% of the maximal velocity [V_{max}] obtained during the baseline incremental treadmill test, 0-15% inclination). For the main part, exercise duration, treadmill speed, and inclination were gradually increased. Thus, the program began at low workloads on the first week (25-33 minutes at 50-55% of V_{max} , 5% inclination) and ended with moderate workloads (30-40 minutes, 70-75% of V_{max} , and 15% inclination). In order to minimize animal discomfort, only gentle back touching (with no electrical stimulation) was used during each training session.

Resistance training

The aerobic training phase was followed by resistance training on 3 days/week (Monday, Wednesday, and Thursday). After several attempts with different resistance exercise modalities [44], we considered that the best option for this mouse model consisted of having the animals grasp a cloth hanger (maintained at 40 cm above a layer of bedding to cushion the falls) while only using the two forepaws for as long as possible (6 attempts interspersed with 10-minute rest periods).

Outcomes

Cardiorespiratory fitness

An incremental treadmill test was used to determine the CRF of the mice following a previously described protocol with slight modifications [42]. Mice were subjected to an initial warm-up period (5 minutes at 5 cm/s and 15% inclination; followed by 5 minutes at 8 cm/s and 15% inclination) after which treadmill speed was increased by 2 cm/s every 2 min (while inclination kept constant at 15%) until exhaustion – that is, until the mice spent more than 5 seconds on the electric grid at the back of the treadmill and were unable to continue running. Electrical stimulation was kept at 0.2 mA/1 Hz during the test. The total

distance (meters) achieved by each mouse was recorded as the CRF (or ‘maximal aerobic capacity’).

Forelimb grip strength

Muscle strength was measured as the maximum force (g) exerted by the mice before losing grip, using an isometric force transducer (Harvard Apparatus) [42] on the day before the treadmill test. Each mouse took the test 3 times with a 5-minute rest period between them, and the best reading was recorded as the maximal grip strength.

Skeletal muscle measures

Frozen skeletal muscle tissues were processed as described elsewhere [45], with ice-cold 10 mM Tris-HCl pH 7.6, containing 150 mM NaCl, 1 mM EDTA, 1% Triton™ X-100 and a protease and phosphatase inhibitor cocktail (Roche Diagnostics Corporation; Indianapolis, IN) 1:10 (weight:volume) in a potter homogenizer. Protein concentration was determined with the Pierce® BCA protein assay kit (Thermo Fisher Scientific; Waltham, MA) according to manufacturers’ instructions.

Tibialis anterior homogenates (20-40 μg) were analyzed through western blotting to determine indicators of aerobic metabolism (citrate synthase [CS] and mitochondrial respiratory chain subunits), anabolic status (ratio of phosphorylated/activated ribosomal protein p70 S6 kinase [pP70S6K] to total P70S6K), and antioxidant defense (catalase, glutathione reductase, mitochondrial superoxide dismutase). Briefly, sodium dodecyl sulfate–polyacrylamide gel electrophoresis was performed on a 7.5-12.5% separation gel. Resolved proteins were transferred to a polyvinylidene difluoride (PVDF) membrane, blocked with a solution of Tris-HCl with Tween 20 0.1% (TBST) with 5% skimmed milk or bovine serum albumin and incubated with primary and peroxidase-conjugated secondary antibodies (Supplemental file 1), which were immunodetected using the ECL Prime Western Blotting Detection Reagent (Amersham GE Healthcare; Little Chalfont, UK) in the image analyzer ChemiDoc™ MP Imaging System (Bio-Rad; Hercules, CA). Band densities were determined by densitometric scanning (Image Lab™ Software, version 5.0., Bio-Rad). Total protein load per lane was determined with Coomassie Blue staining of the PVDF membranes [46].

Survival

Survival was evaluated by counting the time (number of days) elapsed from the start of the intervention until ‘spontaneous’ death (i.e., attributable to the tumor) or end of the study (with the latter corresponding to the end of the 5-day postintervention phase, as previously shown in Figure 1). In addition, based on ethical reasons those mice not dying before the end of the study were sacrificed if showing signs of very poor health status or significant suffering (i.e., severe hunching impairing movement, lack of spontaneous mobility, and facial expression of pain).

Clinical evolution

Mouse body mass was measured and disease severity scored, respectively, in each mouse by the same researcher every weekday during the same (aforementioned) period as survival. A total score was computed on a 0 (absence) to 3 (maximal severity) scale by adding individual scores for the following variables: posture (0 [normal], 0.5 [hunching noted only at rest]) or 1 [severe hunching impairing movement]); fur texture

(0 [normal], 0.5 [mild-to-moderate ruffling], or 1 [severe ruffling/poor grooming]); and activity (0 [normal], 0.5 [mild-to-moderately decreased], or 1 [stationary unless stimulated]) (adapted from [43]).

Metastasis

Representative samples of tumors and other organs (kidneys, liver, gut, pancreas, spleen, lung, and brain) were excised and included in formalin-fixed paraffin-embedded (FFPE) blocks. FFPE samples were sectioned at a 3 μm thickness with a microtome, mounted onto microscope slides and stained with H&E. Morphological evaluation by senior pathologists (FR, SZ) was performed on representative sections from primary tumor and mice organs in order to detect metastatic deposits.

Tumor volume

Tumor volume was calculated upon sacrifice with a digital caliper in two orthogonal dimensions using the following formula: volume (mm^3) = $1/6\pi \times \text{length (mm)} \times \text{width}^2 (\text{mm}^2)$, where tumor length was the greatest dimension of the tumor with the other dimension (at a 90° angle) being taken as the width. Tumors were also weighted upon sacrifice (ME303T/00, Mettler Toledo; Barcelona, Spain).

Tumor immunohistochemistry

For each case, FFPE tumor samples were assessed for markers of apoptosis, cell cycle control, and proliferation. Immunohistochemistry analyses (antibodies described in detail in Supplemental file 2) were performed in 3 μm sections of FFPE tumor tissue using coated microscope slides (FLEX IHC Microscope Slides; Dako Omnis, Agilent; Glostrup, Denmark). The slides were incubated for 1 hour at 56 °C to allow the tumor section to be perfectly adhered before staining. Immunohistochemistry analyses were performed automatically on the Autostainer Link 48 (Agilent) using the EnVision™ + System-HRP (DAB) kit (Dako Omnis) following the manufacturer's instructions.

In some cases (cleaved caspase-3, Ki-67, vascular endothelial growth factor receptor 2 [VEGFR2], and Factor VIII), it was necessary to include an intermediate step in order to amplify the signal through an additional 20-minute incubation with EnVision™ FLEX + Rabbit. Thereafter, HRP staining was visualized with 3,3'-diaminobenzidine tetrahydrochloride in organic solvent (DAB) as chromogen, adding EnVision™ FLEX DAB + Chromogen (Dako Omnis) during 10 minutes, and using hematoxylin reagent (EnVision™ FLEX Hematoxylin, Dako Omnis) for counterstaining during 5 minutes. When the staining was ended, the slides were mounted on the automatic CoverStainer (Dako Omnis). Those slides that were only stained with secondary antibodies were used as negative controls.

Visualization of digital slides and image processing was performed by the Philips system (IntelliSite Image Management System; Philips; Best, NL). The stained sections were evaluated semi-quantitatively by two independent pathologists (FR, SZ) blinded to group assignment. Expression of Ki-67, histone deacetylase 3 and cleaved caspase-3 were evaluated in tumor cells as % of stained cells. Nuclear staining was required for evaluation. The expression levels of VEGFR2 were determined as the % of vessels with positive endothelial cells for VEGFR2 relative to the total number of vessels per a 20x field (with total

vessel number [average of 3 measurements] identified with Von Willebrand Factor-related antigen [commonly known as 'Factor VIII'] staining).

Gene expression in tumor microenvironment

A tumor piece (30 μg) previously preserved at -80°C after dissection was mechanically disrupted and processed for RNA isolation (RNeasy Plus Mini Kit, Qiagen Inc.; Hilden, Germany) and quantification was done using NanoDrop 100 (Thermo Fisher Scientific). cDNA was generated from 1 μg of RNA and reverse transcribed using SuperScript™ VILO™ cDNA Synthesis Kit (Invitrogen, Thermo Fisher Scientific). The following genes were studied using specific murine TaqMan assays (all from Applied Biosystems™; Foster City, CA) for qRT-PCR analysis (7500 Real-Time PCR System, Applied Biosystems™) using glyceraldehyde 3-phosphate dehydrogenase (*Gapdh*; Mm99999915_g1), as the housekeeping gene: chemokine (C-C motif) ligand 2 (*Ccl2*; Mm00441242_m1) and 3 (*Ccl3*; Mm00441259_g1), intercellular adhesion molecule 1 (*Icam1*; Mm00516023_m1), interferon beta 1 (*Ifnb1*; Mm00439552_s1) and gamma (*Ifng*; Mm01168134_m1), interleukin 15 (*Il15*; Mm00434210_m1), metalloproteinase 9 (*Mmp9*; Mm00442991_m1), tumor growth factor beta 1 (*Tgfb1*; Mm01178820_m1), tumor necrosis factor (*Tnf*; Mm00443258_m1), vascular cell adhesion protein 1 (*Vcam1*; Mm01320970_m1), and vascular endothelial growth factor A (*Vegfa*; Mm01281449_m1) and R1 (*Vegfr1*; Mm00438980_m1).

Tumor samples were analyzed in duplicate using 7500 Real-Time PCR software v2.0.6 (Applied Biosystems™). The formula $2^{-\Delta\Delta Ct}$ was used to calculate the relative expression ratio in experimental groups, where all values were normalized to *Gapdh*. Data are presented with respect to non-exercise (control) group.

Immune analyses in tumors and blood

Before analyzing immune infiltrated cells, tumor mass was carefully washed with HBSS 1X and mechanically processed prior to enzymatic digestion with 1 mg/mL of collagenase D (Roche; Catalog #11088858001). Tumor cell suspension was counted by trypan blue and $5 \cdot 10^5$ alive cells were used for immune cell phenotype analysis.

Peripheral and tumor immune cells were studied with flow cytometry. Homogenates of tumor tissue and fresh peripheral blood samples were incubated using appropriate combinations of monoclonal antibodies (Supplemental file 3) at 4°C in the dark for 30 minutes. Red blood cells were lysed using QuickLysis buffer (Cytognos S.L.; Santa Marta de Tormes, Spain) for 30 minutes at room temperature in darkness. A minimum of 20,000 events were acquired in a FACS Canto II cytometer (BD Biosciences; San Jose, CA) and analyzed using FACS Diva software v6.1.2 (BD Biosciences). Details on the procedures used from the moment of tumor sample collection until actual immune cell phenotyping of tumor infiltrates with flow cytometry are shown in Supplemental file 4.

We determined CD45+ cells (commonly known as 'leukocytes'), discerning between myeloid components (macrophages and myeloid-derived suppressor cells [MDSC] [CD11B+], and dendritic cells [CD11C+]), on the one hand, and lymphoid components (T [CD3+], B [B220+], and natural killer [NK] cells [NK1.1+]), on the other. The different T lymphocyte subtypes (helper [CD4+] and cytotoxic T cells

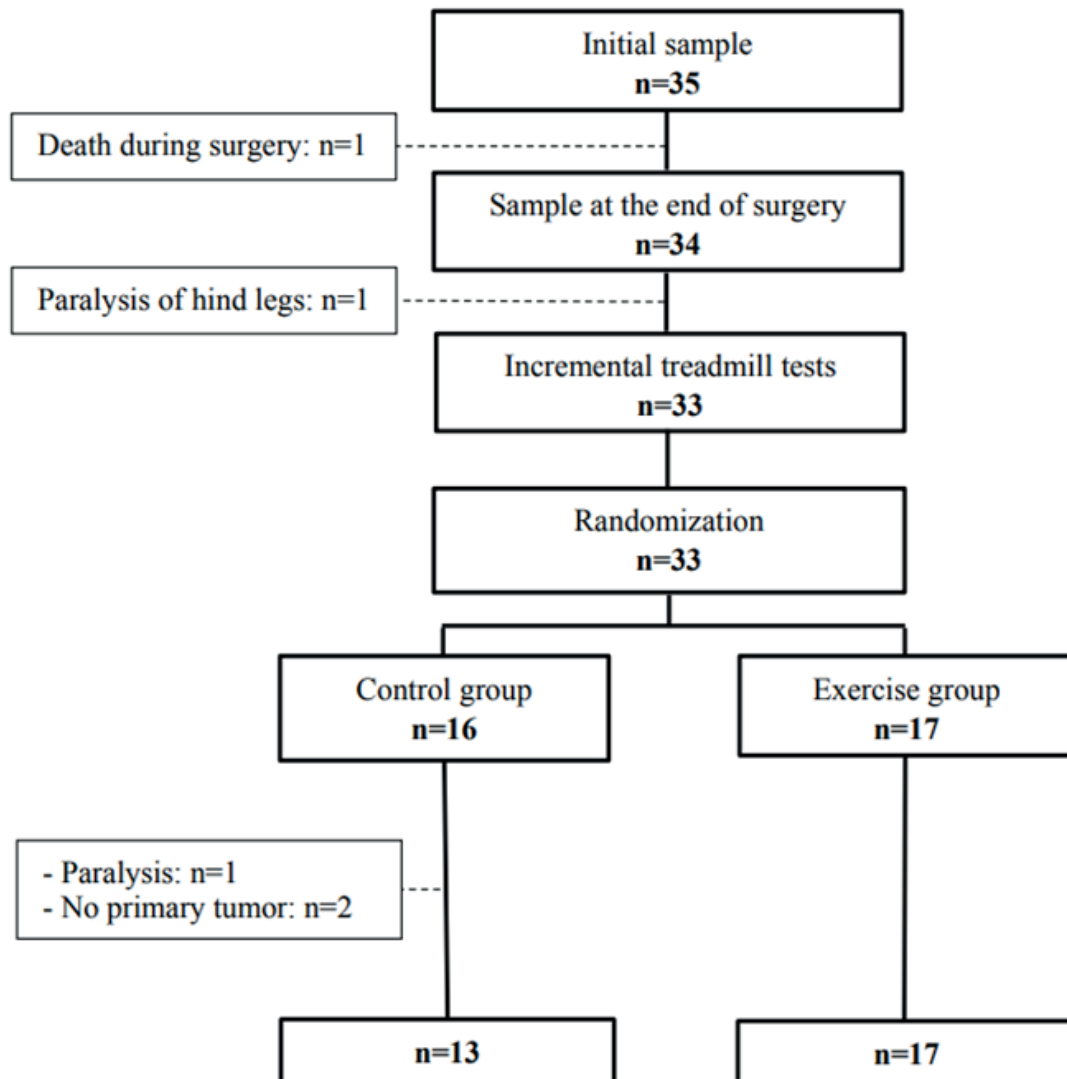


Figure 2. Study flow diagram.

[CD8⁺] were also analyzed. T-cell differentiation was defined as the proportion of naïve (CD4⁺/CD8⁺ CD62L⁺ CD44⁻) and central (CD4⁺/CD8⁺ CD62L⁺ CD44⁺), effector (CD4⁺/CD8⁺ CD62L⁻ CD44⁺) or terminally differentiated effector memory (CD4⁺/CD8⁺ CD62L⁻ CD44⁻), respectively, within the total CD4 or CD8 T-cell population. Recent (OX40⁺, 4-1BB⁺) and sustained lymphocyte activation (programmed cell death 1 [PD1]⁺), lymphocyte-activation gene 3 [LAG3]⁺, and T-cell immunoglobulin and mucin domain-containing protein 3 [TIM3]⁺) states were also analyzed. The two major subsets of MDSC (CD45⁺ CD11B⁺), such as granulocytic (CD11B⁺ Ly6G⁺ Ly6Clow) and monocytic MDSC (CD11B⁺ Ly6G⁻ Ly6Chigh) cells, and M1-like (CD11B⁺ Ly6G⁻ Ly6C⁻ CD206⁻) and M2-like (CD11B⁺ Ly6G⁻ Ly6C⁻ CD206⁺) macrophages were also included in the analysis. Finally, dendritic cells (DCs) were analyzed including the plasmacytoid (CD45⁺ CD11C⁺ CD123⁺) and myeloid (also known as ‘conventional’; CD45⁺ CD11C⁺ CD123⁻) subsets, respectively.

The levels of the following cytokines/chemokines were determined in serum samples at baseline and postintervention using a multiplex Mouse Cytokine Panel (Merck Life Science; Madrid, Spain) based on the Lumine xMAP® technology

on a MAGPIX® instrument (EMD Millipore Corporation; Burlington, MA) according to the manufacturers’ instructions: granulocyte-macrophage colony-stimulating factor (GM-CSF), IFNβ1, IFNγ, IL2, IL6, IL15, macrophage inflammatory protein (MIP)1α, monocyte chemoattractant protein (MCP)1, TNFα, and VEGF.

Statistical analyses

A two-factor (group, time), ANOVA with repeated measures on time was used to determine the effects of the exercise intervention on those outcomes that were measured both at baseline and postintervention (i.e., CRF, forelimb grip strength, and all blood variables [i.e., immune cell phenotypes and cytokines/chemokines]). The Mann Whitney U test was used for unpaired comparisons in those outcomes that were measured only at postintervention (i.e., all skeletal muscle and tumor-related variables). The χ^2 test (or Fisher’s exact test if >20% of the cells in the cross-table had an expected frequency <5) was used for between-group comparisons of the proportion of metastases and ‘hot tumors’, and the Kaplan-Meier analysis (right censored) was used for survival comparisons. On the other hand, whether the pattern of missing data for the different measurements

Table 1. Cardiorespiratory fitness (CRF) and muscle (forelimb) grip strength by group.

Outcome	Group	Baseline	Postintervention	% change	Group (p)	Time (p)	Group by time (p)
CRF (meters)	Control	653 ± 80	193 ± 35	-70 ± 56	0.677	<0.001	0.039
	Exercise	595 ± 72	320 ± 60	-46 ± 17			
Grip strength (grams)	Control	172 ± 6	149 ± 7	-13 ± 17	0.996	0.020	0.792
	Exercise	174 ± 11	151 ± 7	-13 ± 36			

Data are mean ± SEM. Total N with complete data =11 (control) and 12 (exercise).

followed each of three possibilities was also analyzed [47]: a) missing completely at random (i.e., no relationship between the missingness of the data and any values, observed or missing); b) missing at random (i.e., existence of a systematic relationship between the propensity of missing values and the observed data, but not the missing data); and c) missing not at random (also known as ‘non-ignorable missingness’, i.e., the data are neither missing completely at random nor missing at random, with the value of the missing variable related to the reason it is missing).

RESULTS

The initial number of mice before tumor cell inoculation was 35 (Figure 2). One of them died during surgery, another one was excluded as its hind legs were paralyzed before starting the familiarization phase (morbidity associated with the technique = 3%), two did not present the primary tumor into the left para-adrenal space despite showing several masses located in other parts of the body (e.g., abdominal region), and another one showed paralysis in its hind legs during the intervention phase. These mice were not included in the analysis of the results. Therefore, the efficiency of engraftment of the tumor cell line was 94%. The final number of mice completing the study was 13 and 17 in the control and exercise group, respectively.

On the other hand, despite the lack of data for analyses from several mice (as detailed in the Tables and Figures below), the missing data for the different outcomes followed a missing-completely-at-random pattern, which rules out, at least partly, the possibility of inherent bias.

Physical fitness

Physical capacity declined throughout the study in both groups, yet with a significantly attenuation of CRF decline in the exercise group compared with control mice ($p=0.039$ for the group by time interaction effect; Table 1). No changes were found, however, in muscle grip strength.

Skeletal muscle adaptations to training

Higher levels (all $p \leq 0.001$) of several markers of muscle aerobic adaptations (i.e., CS levels, as well as those of respiratory chain complexes III, IV and V) and antioxidant defense (glutathione reductase) were found in the exercise group compared with control mice, although no differences were found for muscle anabolic status indicators (pP70S6K/P70S6K ratio) (Figure 3).

Clinical data

Survival

No significant between-group differences were found in survival (Figure 4), with median values of 28 days (range 11

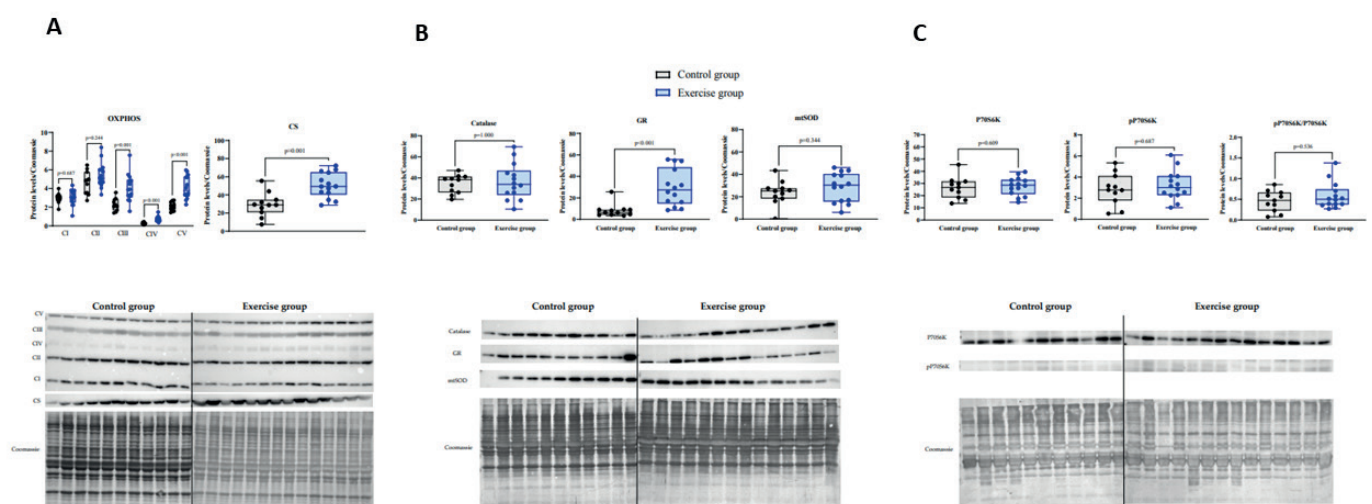


Figure 3. Markers (western blot results) of exercise training adaptations in total skeletal muscle (tibialis anterior) homogenates by group (with total protein content per lane determined by Coomassie Blue 280 staining used as loading control). Data are mean ± SEM and individual data values (N with data = 11 [10-11 for panel B] and 14 in the control and exercise groups, respectively) and p-values for between-group comparisons are also shown. Panel A. Oxidative phosphorylation (OXPHOS) components (mitochondrial respiratory complexes I to V [CI to CV]) and citrate synthase (CS). Of note, the commercial cocktail of antibodies (Supplementary file 1) been used allows to determine all five complexes CI to CV simultaneously. Panel B. Antioxidant defense (catalase, glutathione reductase [GR] and mitochondrial superoxide dismutase [mtSOD]). Panel C. Proteins involved in anabolic status (phosphorylated/activated ribosomal p70 S6 kinase [Thr389] [pP70S6K] and total ribosomal protein p70 S6 kinase [P70S6K]). The ratio of pP70S6K to P70S6K reflects the anabolic status in the analyzed muscle.

to 37) and 25 days (3 to 37) in the exercise and control group, respectively

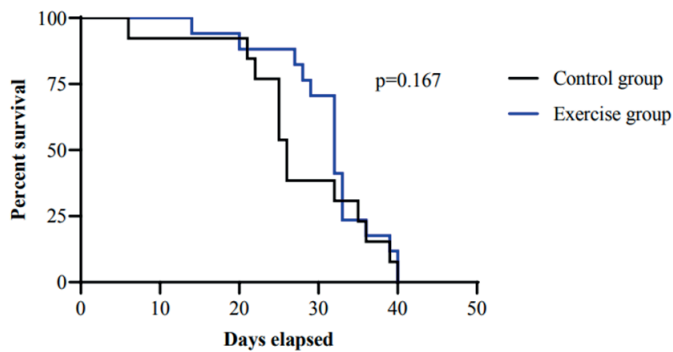


Figure 4. Survival estimates by group (with the p-value for the between-group comparison also shown). Total N with data =13 and 17 for the control and exercise groups, respectively. Survival was evaluated by counting the time (number of days) elapsed from the start of the intervention until death or end of the study (i.e., end of the 5-day postintervention phase previously shown in Figure 1) and therefore the timeframe before the start of intervention (post-surgery recovery phase and baseline measurements, previously explained in Figure 1) is not shown.

Clinical evolution

During the first week after the tumor cell inoculation, a deterioration in health status was noted in all the mice, as reflected by an increase in all individual scores (hair, posture, spontaneous activity). During the following ~2 weeks, however, there was a progressive improvement in health status, with all animals reaching a good recovery level in the different disease evolution parameters before beginning the intervention phase. The same trend was observed for body mass during this period of time (data not shown). From the start of intervention to the end of it, no significant group by time interaction effect (all $p>0.1$) was found for body mass (Figure 5A) or clinical severity (individual/total) scores (Figure 5B).

Tumor development and metastases

Tumor weight and volume

Tumors were palpable ~2 weeks after tumor cell inoculation and thus ~1 week before baseline assessments. Mean tumor volume and weight did not significantly differ between groups at sacrifice (Figure 6).

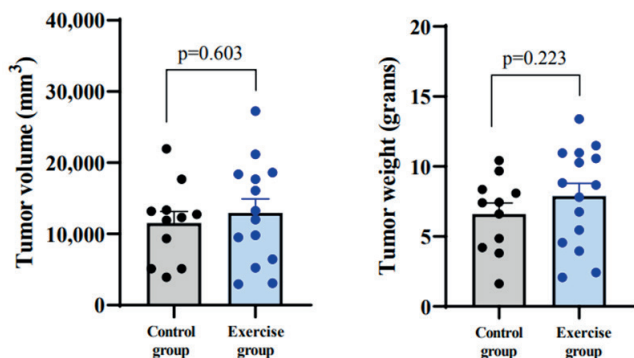


Figure 6. Tumor volume and weight at sacrifice by group. Data are mean \pm SEM. Individual data values and p-values for between-group comparisons are also shown. N with = 11 and 14 (control and exercise group, respectively).

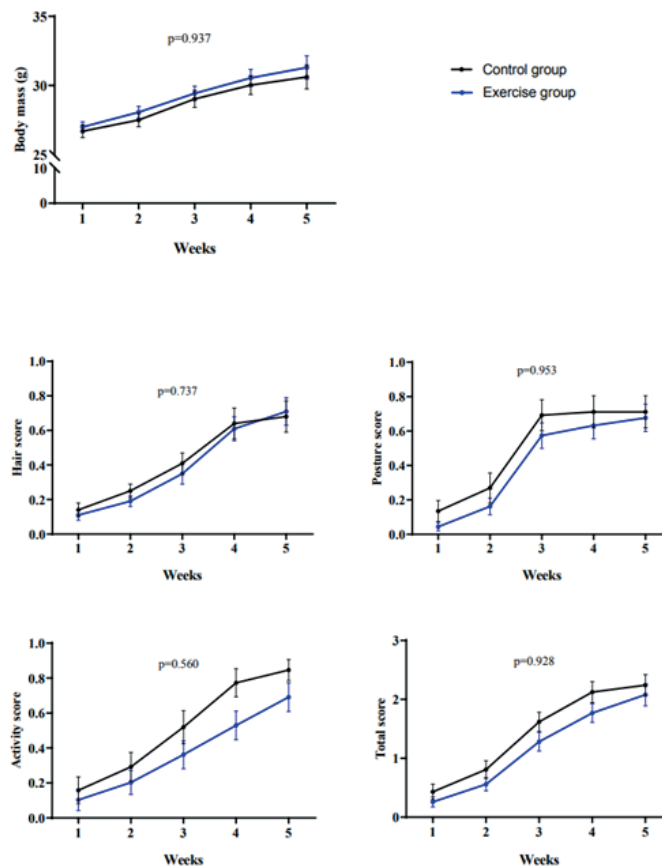


Figure 5. A. Body mass evolution by group from the start to the end of the intervention phase, respectively. No significant group by time effect (two-factor [group, time] ANOVA with repeated measures on time) was found. B) Daily clinical disease progression (individual and total disease severity scores, where a higher score denotes a higher severity) by group from the start to the end of the intervention, respectively. No significant group by time effect (two-factor [group, time] ANOVA with repeated measures on time) was found for individual (hair, posture, activity) or total scores. Data are mean \pm SEM, with p-values for group by time interaction effect shown. N with complete data = 13 and 17 (control and exercise group, respectively).

Metastasis

No significant between-group differences were found for the prevalence of metastatic lesions (Table 2). The tissues most commonly affected by metastasis were the spleen and the liver, accounting for 83% of all metastases for both groups combined, with lung and pancreas metastases (in one mouse of the exercise and control group, respectively), accounting for the remainder of metastases (Figure 7).

Table 2. Metastasis analysis by group and analyzed organ. N with complete data of = 5 (control) and 10 (exercise). The p-value corresponds to the Fisher exact test.

Organ	Group	Mice with metastasis (%)	p-value
Spleen	Control	60%	0.580
	Exercise	33%	
Liver	Control	33%	0.560
	Exercise	20%	
Pancreas	Control	33%	0.095
	Exercise	0%	
Lung	Control	0%	1.000
	Exercise	13%	
Brain	Control	0%	1.000
	Exercise	0%	
Gut	Control	0%	1.000
	Exercise	0%	
Kidneys	Control	0%	1.000
	Exercise	0%	

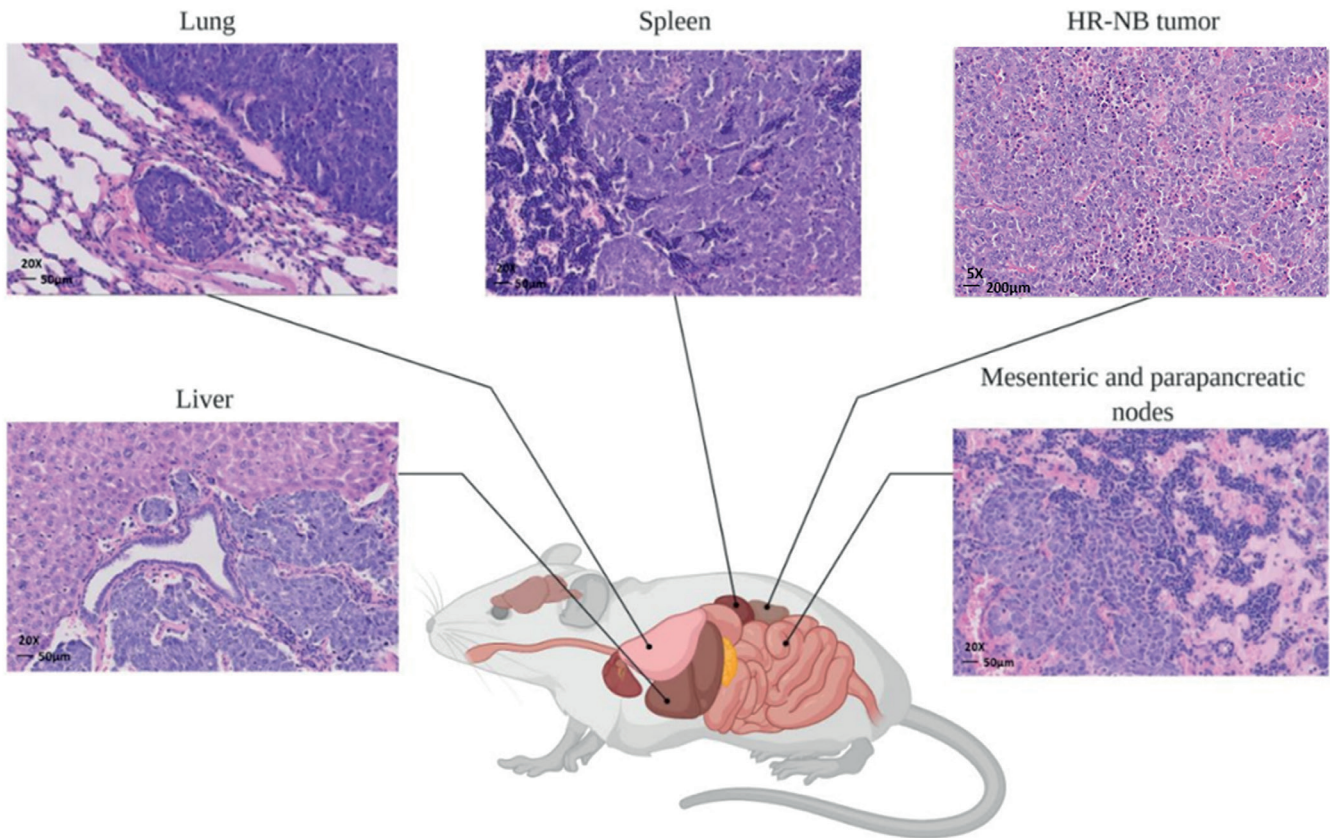


Figure 7. Representative images from hematoxylin and eosin staining of the most commonly affected tissues with metastatic lesions (lung, spleen, liver and pancreas) and the tumor.

Intratumoral studies

Immunohistochemical analyses

H&E staining of the tumors showed a significantly higher proportion of positive cells for the markers of apoptosis and angiogenesis that we studied, caspase-3 ($p=0.029$) and VEGFR2 ($p=0.012$), respectively, in exercised mice compared with controls (Figure 8) – although no between-group differences were found in the total vessel count (26.2 ± 2.2 and 26.8 ± 3.9 per $\times 20$ field, respectively, $p=0.789$). Yet, no significant between-group differences were found for Ki67 ($p=0.240$; with the vast majority of cells [$\geq 96\%$] positive for this marker of proliferation in both groups) or histone 3 deacetylase ($16.0 \pm 2.8\%$ versus $11.9 \pm 1.8\%$ for control and exercise groups, respectively; $p=0.438$).

Gene expression associated with the tumor microenvironment

No significant between-group differences were found for gene expression associated with the tumor microenvironment, although a trend towards higher values of *Tgfb1* expression levels and lower values of *Ccl2* expression levels were observed in the exercise group ($p=0.067$ and $p=0.072$, respectively) (Figure 9).

Immune cell phenotyping

Peripheral blood. Compared to control mice, the exercise group showed a significant increase from baseline to postintervention in the proportion of CD4 naïve T cells compared to controls ($p=0.050$ for the group by time intervention effect) and a similar (albeit nonsignificant) trend was found for the proportion of CD4 T cells expressing markers of recent (OX40) T cell activation ($p=0.093$) and central memory CD4 T cells ($p=0.072$) (Table 3). No significant differences were shown between the groups if data expressed as cell counts (data not shown).

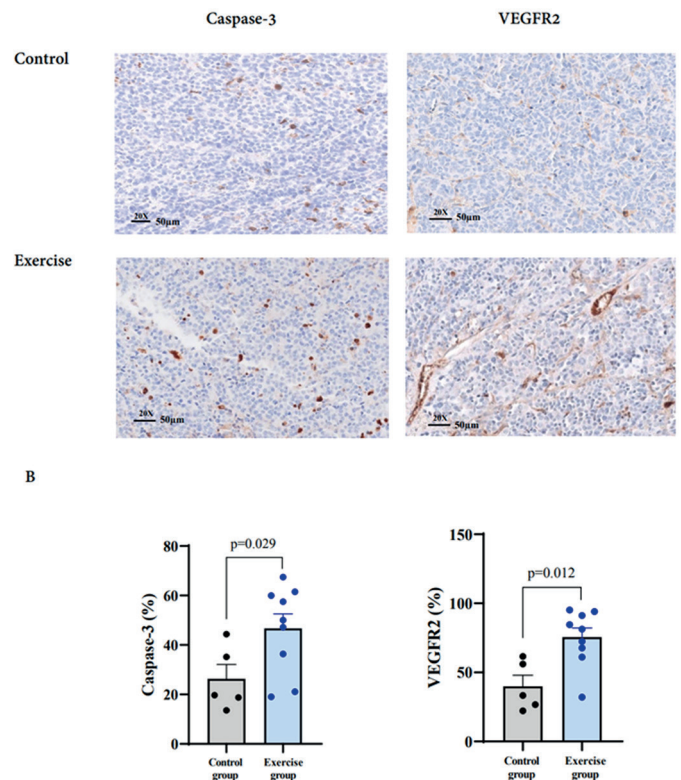


Figure 8. Immunohistochemistry analyses of markers of apoptosis (cleaved caspase 3) or angiogenesis (vascular endothelial growth factor receptor 2 [VEGFR2]) by group. (A) Representative images showing higher caspase-3 and VEGFR2 expression levels, respectively, in a mouse from the exercise group compared with a control. (B) Mean \pm SEM values (together with individual data) expressed as % of positive cells, of these two markers in each group (with p-values for between-group comparisons also shown). N with data = 5 and 9 (control and exercise group, respectively).

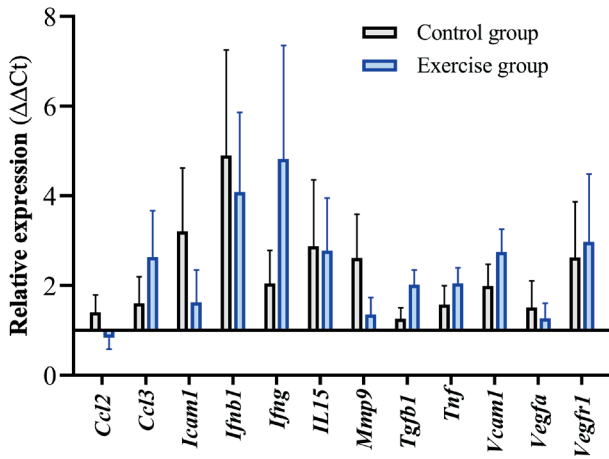


Figure 9. Gene expression analysis (real-time quantitative polymerase chain reaction) in homogenized tumors by group. Abbreviations: *Ccl2*, chemokine (C-C motif) ligand 2; *Ccl3*, chemokine (C-C motif) ligand 3; *Icam1*, intercellular adhesion molecule 1; *Ifnb1*, interferon beta; *Ifng*, interferon gamma; *IL15*, interleukin 15; *Mmp9*, metalloproteinase 9; *Tgfb1*, transforming growth factor beta 1; *Tnfa*, tumor necrosis factor alpha; *Vcam1*, vascular cell adhesion protein 1; *Vegfa*, vascular endothelial growth factor-a; and *Vegfr1*, vascular endothelial growth factor receptor 1. Data are mean ± SEM with relative gene expression calculated as mRNA intratumoral levels normalized to those of the housekeeping gene, glyceraldehyde 3-phosphate dehydrogenase. No significant between-group differences were found (all $p > 0.1$), although a trend to higher values of *Tgfb1* and lower values of *Ccl2* transcripts in the exercise group ($p = 0.067$ and $p = 0.072$, respectively) were observed. N with data = 11 and 14 (control and exercise group, respectively).

Tumors

In flow cytometry analyses, the proportion of ‘hot’ tumors tended to be higher ($p = 0.079$ for Fisher exact test) in the exercise group (76.9% [10 of 13]) compared with control mice (33.3% [3 of 9]) (examples shown in Supplemental file 5). In turn, within ‘hot’ tumors, those from exercised mice showed significantly higher levels of total leukocyte (i.e., CD45+ cells) and myeloid cell infiltrates ($p = 0.045$ and 0.049 , respectively), but not of lymphoid cells infiltrates (Figure 10).

Regarding specific myeloid subpopulations, tumors from exercise mice showed a higher number of M2-like tumor-associated macrophages ($p = 0.028$) and DCs ($p = 0.049$) than the control group, and a trend toward a higher number of myeloid and plasmacytoid DCs ($p = 0.077$ for both subsets) was also found (Figure 11). On the other hand, no significant between-group differences were found for the different lymphoid subsets (Figure 12).

Serum cytokines/chemokines

No significant group by time interaction effect was found for the levels of circulating cytokines/chemokines we studied (Table 4).

Table 4. Serum cytokines/chemokines by group.

Cytokines/chemokines	Group	N	Baseline	Postintervention	Group (p)	Time (p)	Group by time (p)
IL6 (pg/mL)	Control	10	45 ± 8	63 ± 12	0.748	0.819	0.172
	Exercise	8	73 ± 35	48 ± 15			
IL15 (pg/mL)	Control	5	599 ± 313	282 ± 81	0.526	0.351	0.453
	Exercise	5	321 ± 203	285 ± 64			
MCP1 (pg/mL)	Control	5	183 ± 44	172 ± 77	0.300	0.898	0.878
	Exercise	3	87 ± 6	85 ± 31			
TNFα (pg/mL)	Control	4	10 ± 2	7 ± 3	0.753	0.619	0.545
	Exercise	3	10 ± 1	10 ± 6			
VEGF (pg/mL)	Control	9	0.9 ± 0.2	2.8 ± 1.7	0.220	0.712	0.260
	Exercise	5	6.3 ± 5.0	2.6 ± 1.6			

Data are mean ± SEM. Abbreviations: IL, interleukin; MCP, monocyte chemoattractant protein-1; TNFα, tumor necrosis factor α; and VEGF, vascular endothelial growth factor.

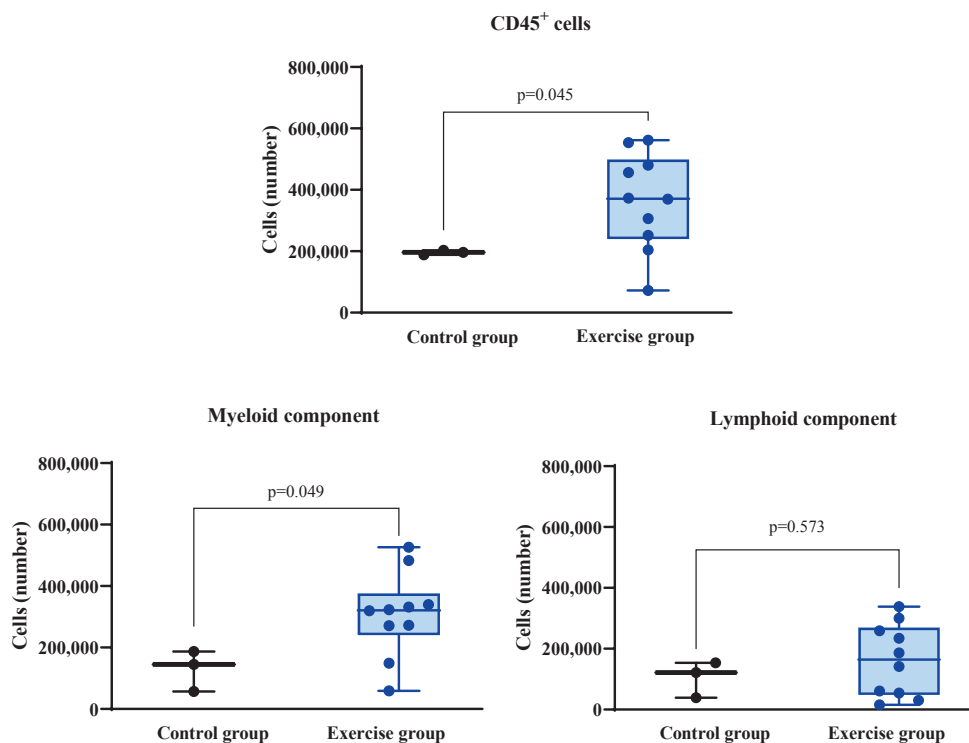


Figure 10. Total leukocyte (i.e., all CD45+ cells), myeloid (macrophages and myeloid-derived suppressor cells [CD11B+], and dendritic cells [CD11C+]), and lymphoid (T [CD3+] and B lymphocytes [B220+], and NK cells [NK1.1+]) infiltrates in ‘hot’ tumors by group. Data are mean ± SEM, with individual data points and p-values for the between group comparison also shown. N with data = 3 and 10 (control and exercise group, respectively).

Table 3. Immune cell phenotyping in peripheral blood by group.

Data are mean (%) ± SEM. Total N with complete data = 6 and 10 for the control and exercise group, respectively. Abbreviations: DCs, dendritic cells; MDSCs, myeloid-derived suppressor cells.

Cell type/subtype (CD markers)	Groups	Baseline	Postintervention	Group (p)	Time (p)	Group by time (p)
Leukocytes (CD45 ⁺)	Control	98.5 ± 0.2	85.7 ± 13.3	0.696	0.078	0.707
	Exercise	98.4 ± 0.3	79.1 ± 10.3			
T lymphocytes (CD45 ⁺ CD3 ⁺)	Control	31.3 ± 2.1	10.0 ± 1.9	0.324	<0.001	0.826
	Exercise	35.7 ± 2.8	13.3 ± 3.5			
B lymphocytes (CD45 ⁺ B220 ⁺)	Control	31.5 ± 1.7	3.5 ± 1.2	0.850	<0.001	0.472
	Exercise	30.1 ± 1.1	4.3 ± 1.6			
Natural killer cells (CD45 ⁺ NK1.1 ⁺)	Control	0.3 ± 0.1	0.1 ± 0.1	0.346	0.002	0.432
	Exercise	0.4 ± 0.1	0.2 ± 0.1			
Myeloid CD11B cells (CD45 ⁺ CD11B ⁺)	Control	27.2 ± 3.6	83.6 ± 3.5	0.372	<0.001	0.536
	Exercise	25.1 ± 2.3	77.6 ± 4.4			
Myeloid CD11C cells (CD45 ⁺ CD11C ⁺)	Control	1.2 ± 0.1	0.6 ± 0.2	0.520	0.416	0.163
	Exercise	1.0 ± 0.2	1.2 ± 0.3			
Lymphoid cell subsets						
CD4 ⁺ T cells (CD45 ⁺ CD3 ⁺ CD4 ⁺)	Control	72.3 ± 1.6	61.6 ± 1.9	0.928	<0.001	0.756
	Exercise	72.0 ± 1.1	62.4 ± 3.0			
CD8 ⁺ T cells (CD45 ⁺ CD3 ⁺ CD8 ⁺)	Control	18.9 ± 0.2	28.2 ± 3.0	0.867	0.001	0.645
	Exercise	19.4 ± 0.5	27.1 ± 2.0			
CD8⁺ T cell differentiation						
Naïve T cells (CD45 ⁺ CD3 ⁺ CD8 ⁺ CD62L ⁺ CD44 ⁻)	Control	0.7 ± 0.2	6.5 ± 2.8	0.753	0.002	0.876
	Exercise	1.0 ± 0.2	7.3 ± 2.0			
Terminally differentiated effector memory T cells (CD45 ⁺ CD3 ⁺ CD8 ⁺ CD62L ⁻ CD44 ⁺)	Control	87.1 ± 1.1	74.2 ± 3.3	0.120	<0.001	0.514
	Exercise	82.9 ± 2.6	67.2 ± 2.8			
Effector memory T cells (CD45 ⁺ CD3 ⁺ CD8 ⁺ CD62L ⁻ CD44 ⁺)	Control	12.1 ± 1.0	19.3 ± 2.6	0.247	0.012	0.833
	Exercise	15.9 ± 2.6	24.3 ± 2.8			
Central memory T cells (CD45 ⁺ CD3 ⁺ CD8 ⁺ CD62L ⁺ CD44 ⁺)	Control	0.6 ± 0.2	1.5 ± 0.8	0.393	0.021	0.453
	Exercise	0.6 ± 0.1	2.2 ± 0.5			
CD8⁺ T cell recent activation						
OX40 (CD45 ⁺ CD3 ⁺ CD8 ⁺ OX40 ⁺)	Control	0.1 ± 0.0	0.4 ± 0.3	0.729	0.090	0.543
	Exercise	0.1 ± 0.0	0.6 ± 0.3			
41BB ⁺ (CD45 ⁺ CD3 ⁺ CD8 ⁺ 41BB ⁺)	Control	0.8 ± 0.5	0.2 ± 0.1	0.500	0.117	0.304
	Exercise	0.4 ± 0.2	0.3 ± 0.1			
CD8⁺ T cell sustained activation						
LAG3 ⁺ (CD45 ⁺ CD3 ⁺ CD8 ⁺ LAG3 ⁺)	Control	0.4 ± 0.2	0.2 ± 0.1	0.174	0.004	0.187
	Exercise	0.2 ± 0.0	0.1 ± 0.0			
TIM3 ⁺ (CD45 ⁺ CD3 ⁺ CD8 ⁺ TIM3 ⁺)	Control	0.6 ± 0.2	0.4 ± 0.1	0.572	0.138	0.835
	Exercise	0.6 ± 0.2	0.2 ± 0.1			
PD1 ⁺ (CD45 ⁺ CD3 ⁺ CD8 ⁺ PD1 ⁺)	Control	3.4 ± 0.3	4.0 ± 0.2	0.217	0.307	0.755
	Exercise	4.1 ± 0.5	4.5 ± 0.5			
CD4⁺ T cell differentiation						
Naïve T cells (CD45 ⁺ CD3 ⁺ CD4 ⁺ CD62L ⁺ CD44 ⁻)	Control	2.3 ± 0.6	1.8 ± 0.8	0.145	0.157	0.050
	Exercise	2.5 ± 0.5	5.1 ± 1.3			
Terminally differentiated effector memory T cells (CD45 ⁺ CD3 ⁺ CD4 ⁺ CD62L ⁻ CD44 ⁺)	Control	76.0 ± 2.3	75.9 ± 4.7	0.506	0.104	0.106
	Exercise	78.1 ± 1.2	68.1 ± 4.4			
Effector memory T cells (CD45 ⁺ CD3 ⁺ CD4 ⁺ CD62L ⁻ CD44 ⁺)	Control	18.7 ± 1.2	20.5 ± 3.7	0.689	0.113	0.323
	Exercise	17.1 ± 1.2	24.6 ± 3.9			
Central memory T cells (CD45 ⁺ CD3 ⁺ CD4 ⁺ CD62L ⁺ CD44 ⁺)	Control	3.9 ± 0.7	2.1 ± 0.7	0.998	0.155	0.072
	Exercise	2.9 ± 0.5	3.2 ± 0.7			
CD4⁺ T cell recent activation						
OX40 (CD45 ⁺ CD3 ⁺ CD4 ⁺ OX40 ⁺)	Control	0.1 ± 0.0	0.0 ± 0.0	0.119	0.147	0.093
	Exercise	0.0 ± 0.0	0.6 ± 0.3			
41BB ⁺ (CD45 ⁺ CD3 ⁺ CD4 ⁺ 41BB ⁺)	Control	0.7 ± 0.3	0.2 ± 0.1	0.811	0.236	0.220
	Exercise	0.4 ± 0.2	0.4 ± 0.2			
CD4⁺ T cell sustained activation						
LAG3 ⁺ (CD45 ⁺ CD3 ⁺ CD4 ⁺ LAG3 ⁺)	Control	0.4 ± 0.1	0.3 ± 0.2	0.263	0.570	0.570
	Exercise	0.2 ± 0.1	0.2 ± 0.1			
TIM3 ⁺ (CD45 ⁺ CD3 ⁺ CD4 ⁺ TIM3 ⁺)	Control	0.7 ± 0.3	0.2 ± 0.1	0.294	0.044	0.475
	Exercise	0.5 ± 0.2	0.2 ± 0.1			
PD1 ⁺ (CD45 ⁺ CD3 ⁺ CD4 ⁺ PD1 ⁺)	Control	7.5 ± 0.8	3.0 ± 0.7	0.074	0.001	0.442
	Exercise	5.9 ± 0.8	2.7 ± 0.4			
Myeloid cells						
Monocytic MDSC (CD45 ⁺ CD11B ⁺ Ly6G ⁻ Ly6C ^{hi})	Control	25.3 ± 3.3	12.6 ± 1.2	0.193	<0.001	0.742
	Exercise	22.5 ± 1.4	11.2 ± 1.2			
Granulocytic MDSC (CD45 ⁺ CD11B ⁺ Ly6G ⁺ Ly6C ^{low})	Control	51.9 ± 5.6	75.6 ± 5.0	0.313	<0.001	0.722
	Exercise	57.1 ± 2.1	77.3 ± 4.2			
Macrophages (CD45 ⁺ CD11B ⁺ Ly6G ⁻ Ly6C ⁻)	Control	22.8 ± 2.8	11.7 ± 4.1	0.632	0.009	0.752
	Exercise	20.3 ± 1.9	11.3 ± 3.6			
M1-like macrophages (CD45 ⁺ CD11B ⁺ Ly6G ⁻ Ly6C ⁻ CD206 ⁻)	Control	99.5 ± 0.1	99.7 ± 0.2	0.478	0.598	0.895
	Exercise	99.4 ± 0.1	99.5 ± 0.4			
M2-like macrophages (CD45 ⁺ CD11B ⁺ Ly6G ⁻ Ly6C ⁻ CD206 ⁺)	Control	0.5 ± 0.1	0.4 ± 0.2	0.654	0.895	0.979
	Exercise	0.6 ± 0.1	0.6 ± 0.4			
Myeloid (conventional) DCs (CD45 ⁺ CD11C ⁺ CD123 ⁻)	Control	91.8 ± 4.3	81.0 ± 7.3	0.210	0.001	0.927
	Exercise	80.5 ± 5.5	70.2 ± 6.0			
Plasmacytoid DCs (CD45 ⁺ CD11C ⁺ CD123 ⁺)	Control	8.2 ± 4.1	19.3 ± 7.5	0.196	0.001	0.896
	Exercise	19.5 ± 5.4	31.3 ± 6.4			

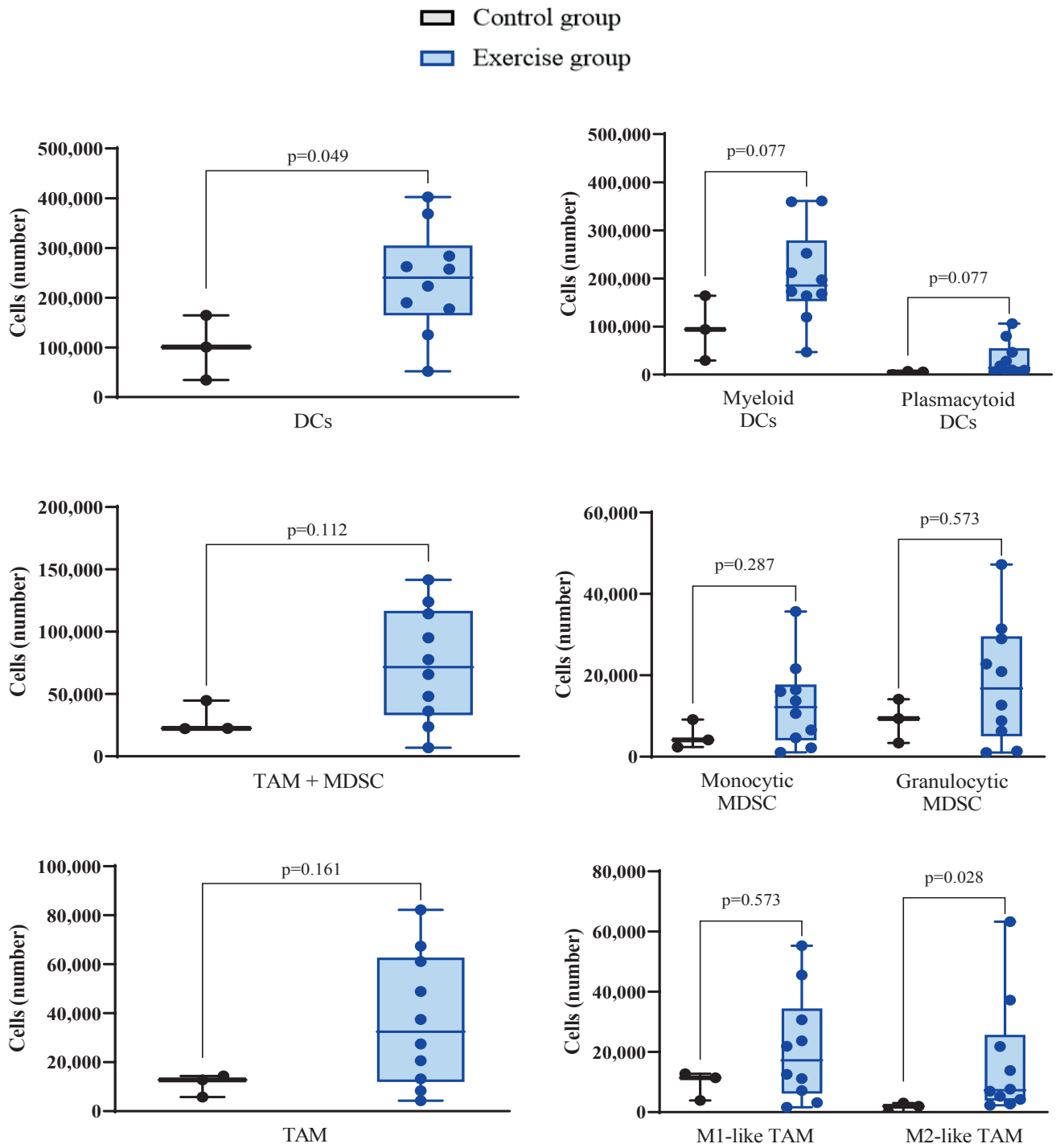


Figure 11. Specific myeloid subpopulation infiltrates in ‘hot’ tumors by study group. Data are mean ± SEM, with individual data points and p-values for between group comparison also shown. N with data = 3 and 10 (control and exercise group, respectively). Abbreviations: DCs, dendritic cells; MDSC, myeloid-derived suppressor cells; TAM, tumor associated macrophages.

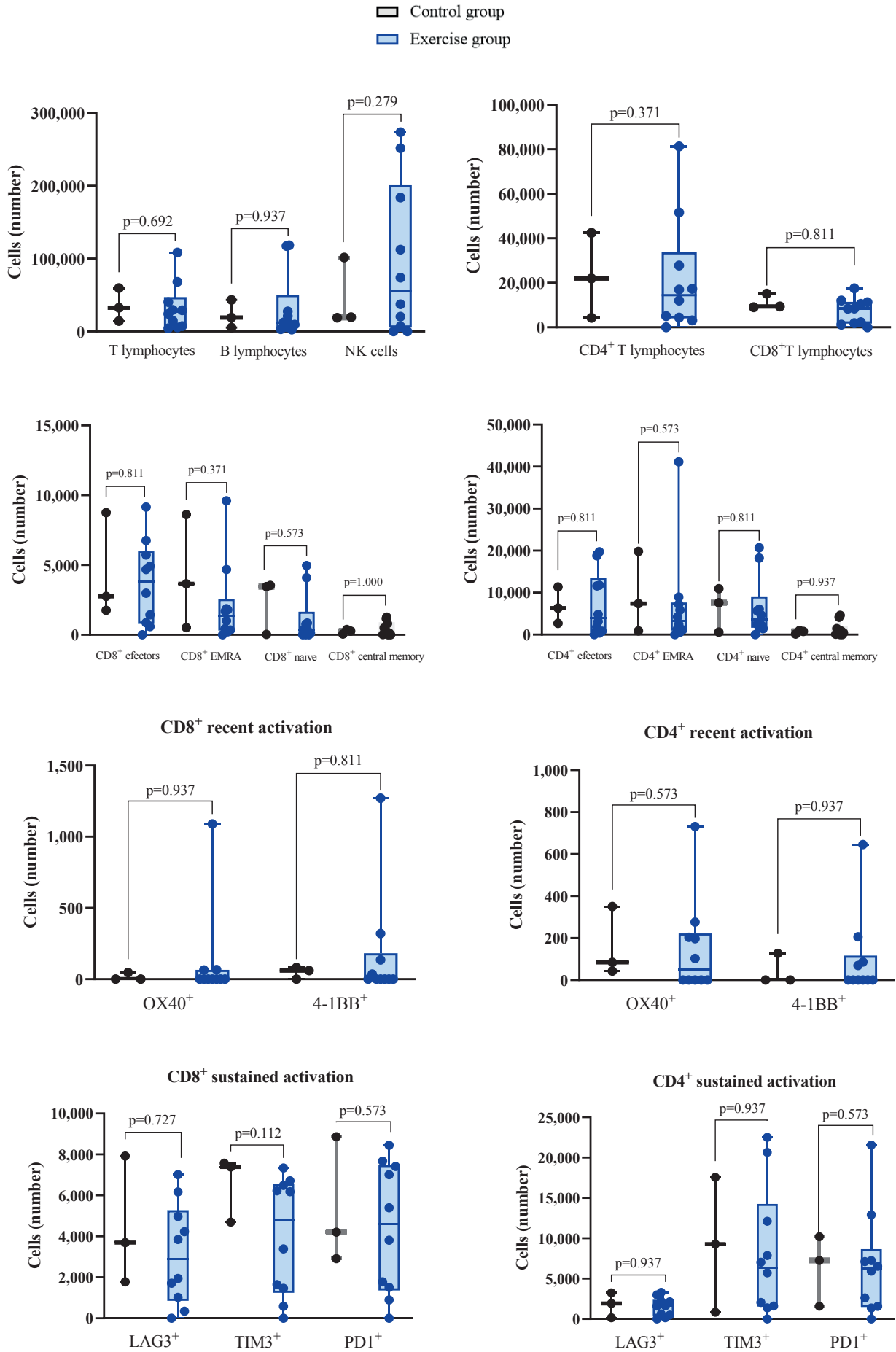


Figure 12. Specific lymphoid subpopulation infiltrates in ‘hot’ tumors by study group. Data are mean ± SEM, with individual data points and p-values for between group comparison also shown. N with data = 3 and 10 (control and exercise group, respectively). Abbreviations: EMRA, terminally differentiated effector memory; NK, natural killer cells.

DISCUSSION

The purpose of this preclinical study was to analyze the effects of a 5-week combined (aerobic and resistance) exercise intervention in the context of a highly aggressive tumor (one of the most treatment-resistant and life-threatening malignancies in children), HR-NB. Of note, because tumors were already palpable ~1 week before baseline measurements, we consider our model to allow studying exercise effects per se (without other concomitant anticancer interventions) after tumor onset (i.e., during the treatment phase) rather than in the prevention setting. Our main finding was that, despite the invasive nature of this tumor (i.e., inducing metastases in ~15% of all the tissues we studied and with a high proliferation rate, as reported by Ki67 results), this type of intervention attenuated the CRF decline associated with this malignancy, which at the muscle molecular level was supported by the finding of higher levels of CS and of several mitochondrial respiratory complexes (together with an improved antioxidant defense) in the exercise group compared with control mice. These exercise-induced benefits were accompanied by significant effects at the tumor tissue level (i.e., higher values of markers of apoptosis [caspase-3] and angiogenesis [VEGFR2] in the exercise group). The program also had an effect on immune cells, at least at the tumor level, with a trend towards a greater proportion of ‘hot-like’ (at least based on flow-cytometry analyses) tumors in the exercise group, together with higher (almost by more than twofold) total levels of tumor infiltrating leukocytes in the ‘hot’ tumors of this group. The latter in turn was partly accounted for by a higher infiltrate of myeloid cells. By contrast, as opposed to previous research in adult preclinical models (see discussion below) no differences were found for lymphoid cell infiltrates in the ‘hot’ tumors. On the other hand, no differences were found for other variables such as cancer progression (tumor volume and weight, metastasis, and tumor microenvironment), clinical severity, or survival, with these results overall expected in the context of an aggressive malignancy.

The exercise-induced benefits on CRF – and on some related variables such as mitochondrial oxidative capacity – in our preclinical model of HR-NB are of potential relevance when extrapolated to patients. In this effect, the benefits of physical exercise on physical function (and particularly CRF) in patients with cancer, particularly adults, are well documented [48,49], and indeed current guidelines recommend that these individuals engage in regular exercise in light of the aforementioned benefits, with subsequent improvements in fatigue and HRQoL [15]. CRF can be impaired in the context of cancer due to different mechanisms, including alterations in cardiac (e.g., cardiotoxicity), pulmonary, or muscle mitochondrial function associated with treatments, all of which are usually aggravated by the low physical activity levels of patients [50]. These adverse effects are not only found in adults, but also in pediatric patients, who typically present with an impaired physical capacity compared with their healthy peers (e.g., Z-score for CRF of -2) [38]. Our finding of an exercise-induced attenuation in CRF decline in the context of HR-NB is of clinical relevance also when considering that CRF levels are inversely associated with the risk of cancer-specific mortality in a dose-response manner [51], and lower levels of CRF have been associated with increased levels of fatigue specifically in children with cancer [38].

Although aerobic training is the exercise modality that has received the greatest attention in the cancer continuum, growing evidence supports the beneficial effects of resistance training, being associated with improvements in muscle strength, body composition (i.e., increased [or at least preserved] muscle mass), and reduced cancer-specific mortality [10,16,52,53]. Muscle strengthening activities represent indeed one of the core recommendations of international guidelines for physical activity [9]. The benefits of strength exercise would be particularly beneficial for patients with HR-NB, as reduced muscle mass has been identified as a predictor of poor prognosis in these individuals [54]. Compared with aerobic exercise, which has been extensively applied in rodents using forced (treadmill running or swimming) or voluntary (wheel running) exercise [12], one of the biggest challenges when implementing a strength training intervention in murine models of disease, particularly cancer, is to quantify and apply optimal training loads such as to induce significant gains in muscle mass and/or function. In this effect, the rapidly increasing tumor volume observed in the HR-NB model used in our study, as well as its location in the abdominal area, made it difficult to choose the right modality and intensity of strength exercise during the intervention. Potentially due to the aforementioned difficulties, no significant intervention effects were found for muscle strength or anabolic status indicators (pP70S6K/ P70S6K).

Physical exercise positively impacts the immune system of healthy people in general [55] with the evidence particularly strong (but not only) for a potential beneficial effect on NK lymphocytes [56-62], which participate in first line innate immune defense through their cytotoxic activity and release of effector cytokines [63]. In fact, a single exercise session suffices to mobilize NK lymphocytes into the bloodstream, although this might not necessarily translate into higher tumor (e.g., prostate) NK infiltrates [60,61]. Interestingly, a recent randomized controlled trial showed in per-protocol analyses higher NK cell infiltrates in tumor infiltration following 8 weeks of intense aerobic training for patients with prostate cancer [64]. However, current meta-analytical evidence does not support a significant long-term effect of exercise training intervention on the circulating levels of these cells or on their ‘static response’ (as assessed in vitro) in cancer patients/survivors [65]. Exercise can also stimulate other immune effectors against tumors beyond NK cells, such as CD8+ (‘cytotoxic’) T cells – which play a crucial role in the control of tumor development [66-69]. Thus, rodent forced running can enhance antitumor immune efficacy by increasing the intratumoral (breast cancer) ratio of CD8+ to CD4+ FoxP3+ T cells (also termed ‘regulatory’ or ‘Treg’, an immune subtype able to induce immune tolerance to tumors) [66]; or restrict tumor growth in multiple murine models of pancreatic ductal adenocarcinoma (PDA) through an expansion of lymphocyte clusters, particularly CD8+ T cells responsive to IL15 signaling (with these cells responsible for the observed reductions in tumor growth) [69]. Of note, patients with PDA who participated in a pre-operative exercise training program showed a significantly higher number of tumor-infiltrating CD8+ T lymphocytes compared with matched historical controls, and higher levels of intratumoral CD8+ T cells in the exercise arm were positively associated with survival [69]. However, other authors have reported no changes with exercise in the tumor infiltrates of mice that were subcutaneously inoculated with PDA cells [70].

One question that has not been addressed in the context of NB is the profile of immune cells infiltrating tumors after exercise training. In this effect, a novel result of our study was that the proportion of ‘hot’ tumors tended to be higher in the exercise group compared to control mice. Furthermore, these tumors showed a higher total immune (leukocyte) and myeloid infiltration compared to control animals. We believe this is a tantalizing finding when considering that the tumor we studied, HR-NB, the most aggressive NB type associated with recurrent somatic mutations and with *MYCN* oncogene amplification, can repress some antigens expressed in tumor cells (such as MCP-1/CCL2, required for chemoattraction of NK cells) and thus impair immune surveillance and immune cell recruitment inside tumors [71]. Indeed, HR-NB with *MYCN* amplification is often characterized by a sparse and limited immune infiltrate in the tumor microenvironment together with lower IFN pathway activation and chemokine expression, and infiltrating immune cells lack activation markers [72-74]. As such, the HR-NB tumor environment is often referred to as ‘cold’ or ‘immune-deserted’ [72]. NB tumors display low immunogenicity due to their low mutational load and lack of major histocompatibility complex class I (MHC-I) expression, with tumor infiltration by T and NK cells especially low in HR-NB and prognostic for survival [75]. Moreover, NB tumors employ a variety of immune evasion strategies that reduce infiltration and reactivity of immune cells (including DCs, as explained below), such as expression of immune checkpoint molecules, induction of immunosuppressive myeloid and stromal cells, as well as secretion of immunomodulatory mediators [75].

The higher total immune (leukocyte) and myeloid infiltration in the tumors of the exercise group compared to control animals was partly accounted for by a higher number of a myeloid subset, DCs. This result is potentially relevant since the presence of tumor-infiltrating DCs is a favorable prognostic immune signature of NB tumors in general, independent from other variables used to stage and stratify treatment of patients such as *MYCN* amplification status or age at diagnosis [76]. Furthermore, NB tumors are able to induce DC dysregulation at multiple levels by inhibiting the maturation and function of these cells [77]. For instance, NB can induce DC dysfunction through inhibition of generation/differentiation of functionally active DCs by NB-derived gangliosides [78] (i.e., glycosphingolipids present on the surface of cells that are implicated in cancer development and progression, including tumor proliferation, invasion, angiogenesis, and metastasis [79]) or decreases in CD40 signaling (a stimulator of DC maturation and antitumor activity) [80] or other soluble factors [81]. In turn, DCs play an important role in anti-tumor immunity – notably in the context of NB – as they act as ‘professional antigen-presenting cells’ involved in initiating and coordinating the immune response against cancer, activating both adaptive (T cell-mediated) and innate (NK cell-mediated) arms of the cellular immune response cascade [82]. Within several tumors, myeloid DCs stimulate and expand tumor-specific effector T cells through IL12 signaling, with a high number of this type of DCs detected in spontaneous regressing tumor models – which suggests they might play a critical role for robust tumor control [83,84]. In turn, plasmacytoid DCs can activate NK cells and are efficient at killing HR-NB [85], which supports the use of immunotherapy with these cells as a potential strategy to decrease the risk of relapse in patients with HR-NB [86]. DCs represent indeed

a potential immunotherapy to promote NB tumor regression, where there are some vaccines involving specific types of the cells that can be used to prevent this malignancy, as well as the combination of inflammatory factors and DCs as a substitute for chemotherapy [87].

In line with our results, Bianco et al. [88] found that an exercise (swimming) intervention increased intratumoral DC infiltrates in a mouse model of breast cancer compared to a non-trained group with the phenotype of these cells also different (i.e., higher CD80 and CD86 expression), suggesting that exercise training could influence the innate immune response to induce DC maturation and promote host antitumor immunity in the tumor microenvironment by presenting tumor antigens. Unfortunately, in our study we did not assess the maturity of the DCs. In any case, we found a trend towards a preferential mobilization of both plasmacytoid and myeloid DCs, with the latter being critical initiators of antitumor T cell responses [77]. On the other hand, the presence of immunosuppressive cells like total TAM, MDSCs, and T regulatory cells in tumors, for which we found no between-group differences in our study, correlate with poor clinical outcomes in NB [89,90].

While keeping in mind the limitation that we did not perform immunohistochemistry studies in TAM beyond flow cytometry analyses, an apparently unexpected, counterintuitive finding was the higher number of a specific subset of TAM, those with an M2-like phenotype, in the ‘hot’ tumors of exercised mice. Nonetheless, recent studies have reported overall comparable findings with regard to TAM in mouse models of breast (91) and lung cancer (92), where exercise in fact inhibited tumor growth, and this beneficial effect was independent of TAM infiltrates (92). Traditionally, macrophages are activated towards one of two polarization states, the classically activated M1 proinflammatory phenotype or the alternatively activated M2 immunosuppressive phenotype. Classically activated M1-like TAM induced by IFN γ and lipopolysaccharides are considered anti-tumor macrophages due to the expression of inducible nitric oxide synthase and the secretion of cytotoxic reactive oxygen species and proinflammatory cytokines, whereas TAM activated by IL4, the so-called M2 TAM, might be considered protumorigenic due to the expression of growth-promoting, proangiogenic, and extracellular matrix remodeling signals via VEGF, among other factors [93]. Importantly, M2-like TAM are also associated with a nonimmune stimulatory phagocytosis of apoptotic cancer cells known as ‘efferocytosis’ [94]. Other ‘professional’ phagocytes (such as monocytes and DCs) and ‘non-professional’ phagocytes (such as epithelial cells) can also participate in efferocytosis [94]. In this effect, the increase in apoptosis of tumor cells induced by the exercise program (as reflected by the higher levels of caspase-3 in the tumors of exercised mice compared to control animals) might explain, at least partly, the greater infiltrates of M2-like TAM inside the ‘hot’ tumors of the intervention group compared to control mice, as well as the increase in myeloid cells in general and DCs in particular (i.e., theoretically to induce efferocytosis).

Our findings are overall in line with the growing evidence on the benefits of physical exercise for improving immune cell effectors [13], albeit different types of cells can be mobilized into the tumors depending on factors such as the exercise protocol (i.e., acute bout versus regular exercise training) or the type of tumor, with scarce evidence up to date translatable to pediatric solid tumors. For instance, a preclinical study reported

that physical exercise promoted the infiltration of immune cells (NK cells in particular) into several types of adult tumors by enhancing the expression of ligands for NK cell-activating receptors (e.g., NKG2D), which seemed dependent on acute exercise-induced release of epinephrine (which increased mobilization of these cells into the bloodstream) and IL6 (which ultimately increased NK cell infiltration into tumors) [95]. In the same line, exercise has been reported to improve the antitumoral activity of resident macrophages [12], reducing the tumor-induced accumulation of MDSC [96,97] or increasing neutrophil infiltrates into tumors [42]. There is also evidence that aerobic or resistance training during chemotherapy can attenuate the immunosuppressive effects of drugs in patients with breast cancer, at least on CD8⁺ cells [98], which correlates well with the aforementioned preclinical evidence that exercise can stimulate CD8⁺ cells to infiltrate tumors [66–69]. In any case, all of the aforementioned studies were conducted in adult tumors, which might explain, at least partly, the fact that we found no between-group differences in CD8⁺ lymphocyte infiltrates. On the other hand, the finding of a significantly higher proportion of circulating CD4 naïve T lymphocytes in our exercise group is overall in line with previous data in humans showing ‘younger looking’ T-cell profiles in physically trained compared to inactive individuals, with overall fewer T-cells exhibiting phenotypes associated with differentiation and exhaustion, and greater frequencies of naïve T-cells and/or recent thymic emigrants that are capable of responding to novel antigens [99–101].

The exercise intervention had a significant effect on two important variables with a major influence in cancer prognosis in general, tumor angiogenesis and apoptosis, with changes in both outcomes potentially explaining some of the biological effects of exercise against cancer development [102]. We found a potential increase in tumor angiogenesis capacity (as reflected by a higher % of VEGFR2-positive vessels inside the tumors despite no differences in total vessel count) with exercise training, which correlates with the aforementioned result for M2-like TAM and the overall proangiogenic effect of these cells [93]. Although there is no unanimity on the effects of exercise on tumor angiogenesis in general [12], emerging data indicates that both acute and chronic (repeated) aerobic exercise stimulate favorable improvements in intratumoral perfusion/vascularization and hypoxia in orthotopic models of human breast cancer and murine prostate cancer [103–105]. Moreover, studies using mouse models of cancers primarily found in the adult population (melanoma, pancreatic, breast, and prostate cancer) have demonstrated that exercise can remodel tumor vasculature and improve chemotherapy efficacy by increasing drug delivery [103–108]. In fact, a preclinical study found that exercise remodeled the vasculature of Ewing sarcoma to reduce vessel hyperpermeability and hypoxia, potentially via modulation of endothelial cell sphingosine-1-phosphate receptors 1 and 2, thereby improving doxorubicin delivery to tumors [23]. Thus, exercise may promote a shift towards a more ‘normalized’ tumor microenvironment (possibly via upregulation of regional and local physiologic angiogenesis) [109].

Controversy exists on the potential direct antitumoral effects of physical exercise in adult cancers. A potential mechanism might be the release of myokines from muscles associated with exercise or ‘exerkines’ (i.e., ‘signalling molecules released from

different tissues in response to acute and/or chronic exercise, which exert their effects through endocrine, paracrine and/or autocrine pathways’ [110] in general). In this effect, we found no changes associated with the intervention in the blood levels of several exerkines (IL6, IL15, or VEGF), or of cytokines/chemokines associated with cancer development (MCP1 [111]) or cancer-related inflammation (TNF α [112]). There is some evidence that ‘exercise-conditioned’ serum might reduce tumor growth *in vitro* [113] (e.g., prostate cancer [114–116]), as first demonstrated by Rundqvist et al. [117]. However, other studies have failed to find such benefits after exercise training, even in the case of serum obtained immediately after an acute exercise bout [118,119]. There is also mixed evidence as to whether exercise training could reduce tumor growth *in vivo*, as reflected by two recent meta-analyses with conflicting results on the effects of physical exercise on tumor growth and metastasis in preclinical models [11,120]. In accordance with the present study, in which no exercise benefits were found on tumor weight or metastasis, other studies have also failed to find beneficial effects of physical exercise on tumor progression. Woods et al. [121] reported no significant differences in breast cancer tumor growth among mice randomized to 14 days of treadmill running compared with sedentary controls. Jones et al. [103] found that breast tumors grew at comparable rates in exercising and sedentary animals. The same group also found that exercise did not inhibit primary cancer progression in an orthotopic model of murine prostate cancer, although it did favorably alter genes responsible for metastatic dissemination in the primary tumor with a shift toward a suppression of distant metastases [104]. On the other hand, other preclinical studies have found a decrease in tumor growth with exercise training [66–69,95,102,122–124], and therefore further research is needed to confirm our findings, as well as to elucidate whether the tumor itself (e.g., not only type, but also method and timing of implantation), the exercise intervention (e.g., timing of exercise initiation, exercise type or intensity) or animal characteristics (e.g., immune deficient versus immune competent versus transgenic) could condition these effects. Notably, studies with the same tumor (B16-F10 melanoma) have reported increased or unchanged intratumoral NK infiltrates if the exercise intervention started before [95] or after [125] implantation, respectively, thereby suggesting that a ‘pre-conditioning effect’ prior to tumor onset may be needed to enhance NK cell infiltration. There is also high variability in the exercise training dose across preclinical studies, and although it is assumed that the same treadmill velocity would fit all mouse strains and experimental conditions, the relative exercise intensity for instance differs between C57BL/6 and Friend Virus B (FVB) female mice (67). This may explain, at least in partly, why preclinical studies can show different results even with similar exercise protocols (7,52,56). On the other hand, the epidemiological evidence for human cancers refers mainly to regular physical activity (e.g., walking or brisk walking) whereas supervised regular exercise (defined as a ‘subset of physical activity that is planned, structured and repetitive and has the objective of improving or maintaining physical fitness’), which was the model used in our study (i.e., mouse forced treadmill running) is a proxy but not a perfect surrogate for physical activity and is thought to induce more profound molecular adaptations than physical activity [12]. In fact, the exercise doses used in preclinical studies might exceed human behavior [67].

No between-group differences were found for the gene expression associated with the tumor microenvironment, with a quasi-significant trend towards higher values of *Tgfb1* transcript levels in the intervention group ($p=0.067$). TGF- β is a member of a multifunctional cytokine family that is involved in essentially all aspects on cancer. On the one hand, TGF- β regulates cell proliferation [126]. TGF- β 1, the most common isoform in human cancers, inhibits proliferation and induces apoptosis in various normal and premalignant human epithelial cells and its essential signaling intermediates (T β RII and Smad4), are therefore considered tumor suppressors. The anti-oncogenic function of this pathway is supported by the frequent occurrence in cancer cells of genetic and epigenetic alterations that abolish its growth-inhibitory function [127]. Interestingly, TGF- β 1 is also considered a myokine, although it primarily induces paracrine effects (that is, in proximity to muscle cells) [110]. On the other hand, however, all advanced human tumors overproduce TGF- β , whose autocrine and paracrine actions in most instances promote tumor growth, invasion, and metastasis [128]. TGF- β also suppresses proliferation and differentiation of lymphocytes, including cytolytic T cells, NK cells and macrophages, thus preventing effective eradication of the developing tumor by the host immune system [127].

Some limitations of the present study should be acknowledged, such as the small sample size available for several outcomes. Due to ethical reasons we could not study very young mice (i.e., aged <2-3 weeks), which would have mimicked the very early occurrence of NB in children's life, and we could not assess acute exercise effects at the blood or tumor level in order to avoid sacrificing an excessive number of animals. For similar ethical reasons, we did not perform additional blood sampling between baseline assessments and the end of the intervention (i.e., before the tumors had grown significantly) and thus we cannot discard that a certain immunosuppressive effect of increasing tumor burden may have attenuated potential exercise benefits. On the other hand, we did not assess the effects of the exercise intervention on immune cells in the absence of tumor burden (i.e., in healthy mice). In turn, a major strength is having analyzed exercise effects in a preclinical model of a pediatric cancer, for which scarce evidence exists compared with adult cancers. Indeed, we have used a very aggressive tumor model developed by our group for which there is only one previous published study [40], where it was shown that these tumors are responsive to mCelyvir (i.e., autologous mesenchymal cells that carry an oncolytic adenovirus inside and is considered a form of cancer immunotherapy). In addition, we assessed a comprehensive range of outcomes. Other strengths and novelties include the use of a flow diagram (which precludes showing data from 'convenient samples') and resistance training in mice, and particularly, the tumor model we used, which allows to recapitulate the main features shown in patients. Indeed, we used an induced HR-NB model in which tumor cells are orthotopically implanted in the suprarenal area of 129/SvJ wild type mice [128,129]. Thus, tumor develop in a fully immunocompetent host, with the appropriate tissue microenvironment, mimicking the conditions that allow the interaction of the immune system with the developing tumor [130].

In summary, although no benefits were observed in tumor progression, clinical severity or survival rates, the present study support the effectiveness of a combined exercise intervention

(aerobic + strength) for attenuating physical function decline in a mouse model of HR-NB, also exerting some immune benefits within the tumor (see Graphical Abstract for a summary of the main study findings). Thus, these findings shed new insights into the potential role of exercise as a potential co-adjuvant therapy in pediatric patients with solid tumors, as well as of potential differences in immune responses compared to adult malignancies.

Funding: Research in pediatric/adolescent cancer by Alejandro Lucia and Carmen Fiuza-Luces is funded by: 'the Wereld Kanker Onderzoek Fonds (WKOF), as part of the World Cancer Research Fund International grant program (grant # IIG_FULL_2021_007), the Spanish Ministry of Science and Innovation (Fondo de Investigaciones Sanitarias [FIS]) and co-funded by the European Union; and the Spanish Ministry of Science and Innovation (Instituto de Salud Carlos III, postdoctoral contract Miguel Servet, # CP18/00034) and Fundación Unoentrecienmil (grant number 2018/10). Research in pediatric/adolescent cancer by Steven J, Fleck and Carmen Fiuza-Luces is funded by a grant from the National Strength and Conditioning Association (NCSA) Foundation (Grant No. PS.1816). This study was also funded by the Spanish Instituto de Salud Carlos III through the project PI20/00147, and co-funded by the European Union Pedro L. Valenzuela is supported by a post-doctoral contract ('Sara Borrell') granted by Instituto de Salud Carlos III (CD21/00138). Cecilia Rincón-Castanedo is supported by a pre-doctoral contract granted by Cecilia Rincón-Castanedo is supported by a pre-doctoral contract granted by Spanish Ministry of Education, Culture and Sport (FPU16/03956). Manuel Ramírez is funded by Fundación Pablo Ugarte, Asociación NEN and Fundación Neuroblastoma.

Conflict of interest: The authors declare no conflicts of interest.

REFERENCES

- 1 Moore, S.C. et al. (2016) Association of Leisure-Time Physical Activity With Risk of 26 Types of Cancer in 1.44 Million Adults. *JAMA Intern. Med.* 176, 816–25
- 2 Matthews, C.E. et al. (2020) Amount and Intensity of Leisure-Time Physical Activity and Lower Cancer Risk. *J. Clin. Oncol.* 38, 686–697
- 3 Lakoski, S.G. et al. (2015) Midlife Cardiorespiratory Fitness, Incident Cancer, and Survival After Cancer in Men: The Cooper Center Longitudinal Study. *JAMA Oncol.* 1, 231–7
- 4 Sanchis-Gomar, F. et al. (2015) Physical inactivity and low fitness deserve more attention to alter cancer risk and prognosis. *Cancer Prev. Res. (Phila).* 8, 105–10
- 5 Morishita, S. et al. Effect of Exercise on Mortality and Recurrence in Patients With Cancer: A Systematic Review and Meta-Analysis. *Integr. Cancer Ther.* 19, 1534735420917462
- 6 Cannioto, R.A. et al. (2021) Physical Activity Before, During, and After Chemotherapy for High-Risk Breast Cancer: Relationships With Survival. *J. Natl. Cancer Inst.* 113, 54–63
- 7 Salam, A. et al. (2022) Effect of post-diagnosis exercise on depression symptoms, physical functioning and mortality in breast cancer survivors: A systematic review and meta-analysis of randomized control trials. *Cancer Epidemiol.* 77, 102111
- 8 Li, T. et al. (2016) The dose-response effect of physical activity on cancer mortality: findings from 71 prospective

- cohort studies. *Br. J. Sports Med.* 50, 339–45
- 9 Bull, F.C. et al. (2020) World Health Organization 2020 guidelines on physical activity and sedentary behaviour. *Br. J. Sports Med.* 54, 1451–1462
- 10 Momma, H. et al. (2022) Muscle-strengthening activities are associated with lower risk and mortality in major non-communicable diseases: a systematic review and meta-analysis of cohort studies. *Br. J. Sports Med.* DOI: 10.1136/bjsports-2021-105061
- 11 Eschke, R.-C.K.-R. et al. (2019) Impact of Physical Exercise on Growth and Progression of Cancer in Rodents-A Systematic Review and Meta-Analysis. *Front. Oncol.* 9, 35
- 12 Ruiz-Casado, A. et al. (2017) Exercise and the Hallmarks of Cancer. *Trends in cancer* 3, 423–441
- 13 Fiuza-Luces, C. et al. (2021) Exercise Benefits Meet Cancer Immunosurveillance: Implications for Immunotherapy. *Trends in cancer* 7, 91–93
- 14 Hanahan, D. and Weinberg, R.A. (2011) Hallmarks of cancer: the next generation. *Cell* 144, 646–74
- 15 Schmitz, K.H. et al. (2019) Exercise is medicine in oncology: Engaging clinicians to help patients move through cancer. *CA. Cancer J. Clin.* 69, 468–484
- 16 Fuller, J.T. et al. (2018) Therapeutic effects of aerobic and resistance exercises for cancer survivors: a systematic review of meta-analyses of clinical trials. *Br. J. Sports Med.* 52, 1311
- 17 Fiuza-Luces, C., Valenzuela, P.L., Morales, J.S. and Lucia A. (2003) Childhood cancer: exercise is medicine. *Lancet Child Adolesc Health* 7, 3–4
- 18 Morales, J.S. et al. (2020) Exercise Interventions and Cardiovascular Health in Childhood Cancer: A Meta-analysis. *Int. J. Sports Med.* 41, 141–153
- 19 Morales, J.S. et al. (2018) Exercise training in childhood cancer: A systematic review and meta-analysis of randomized controlled trials. *Cancer Treat. Rev.* 70, 154–167
- 20 Shi, Q., Zheng, J. and Liu, K. (2022) Supervised Exercise Interventions in Childhood Cancer Survivors: A Systematic Review and Meta-Analysis of Randomized Controlled Trials. *Children* 9, 824
- 21 Bernal, J. et al. (2023) Physical Activity for Cancer-Related Cognitive Impairment Among Individuals Affected by Childhood Cancer: A Systematic Review and Meta-Analysis. *Lancet Child Adolesc Health* 7, 47–58
- 22 Wurz, A. et al (2021) The international Pediatric Oncology Exercise Guidelines (iPOEG). *Transl. Behav. Med.* 11, 1915–22
- 23 Morrell, M.B.G. et al. (2019) Vascular modulation through exercise improves chemotherapy efficacy in Ewing sarcoma. *Pediatr. Blood Cancer* 66, e27835
- 24 Sweet-Cordero, E.A. and Biegel, J.A. (2019) The genomic landscape of pediatric cancers: Implications for diagnosis and treatment. *Science* 363, 1170–1175
- 25 Brodeur, G.M. (2003) Neuroblastoma: biological insights into a clinical enigma. *Nat. Rev. Cancer* 3, 203–16
- 26 Kloc, M., Ghobrial, R.M., Kuchar, E., Lewicki, S. and Kubiak, J.Z. (2020) Development of child immunity in the context of COVID-19 pandemic. *Clin. Immunol.* 217, 108510
- 27 Hsieh, M.H. et al. (2009) Increasing incidence of neuroblastoma and potentially higher associated mortality of children from nonmetropolitan areas: analysis of the surveillance, epidemiology, and end results database. *J. Pediatr. Hematol. Oncol.* 31, 942–6
- 28 Irwin, M.S. and Park, J.R. (2015) Neuroblastoma: paradigm for precision medicine. *Pediatr. Clin. North Am.* 62, 225–56
- 29 Kaatsch, P. (2010) Epidemiology of childhood cancer. *Cancer Treat. Rev.* 36, 277–85
- 30 Matthay, K.K. et al. (2016) Neuroblastoma. *Nat. Rev. Dis. Prim.* 2, 16078
- 31 Colon, N.C. and Chung, D.H. (2011) Neuroblastoma. *Adv. Pediatr.* 58, 297–311
- 32 London, W.B. et al. (2005) Evidence for an age cutoff greater than 365 days for neuroblastoma risk group stratification in the Children’s Oncology Group. *J Clin Oncol* 23, 6459–6465
- 33 Cohn, S.L. et al. (2009) The International Neuroblastoma Risk Group (INRG) classification system: an INRG Task Force report. *J. Clin. Oncol.* 27, 289–97
- 34 Davidoff, A.M. (2012) Neuroblastoma. *Semin. Pediatr. Surg.* 21, 2–14
- 35 Ahmed, A.A. et al. (2017) Neuroblastoma in children: Update on clinicopathologic and genetic prognostic factors. *Pediatr. Hematol. Oncol.* 34, 165–185
- 36 Smith, V. and Foster, J. (2018) High-Risk Neuroblastoma Treatment Review. *Child. (Basel, Switzerland)* 5, 114
- 37 Johnsen, J.I. et al. (2019) Neuroblastoma-A Neural Crest Derived Embryonal Malignancy. *Front. Mol. Neurosci.* 12, 9
- 38 Braam, K.I. et al. (2016) Cardiorespiratory fitness and physical activity in children with cancer. *Support. Care Cancer* 24, 2259–2268
- 39 Dyer, M.A. (2004) Mouse models of childhood cancer of the nervous system. *J. Clin. Pathol.* 57, 561–76
- 40 Franco-Luzón, L. et al. (2020) Systemic oncolytic adenovirus delivered in mesenchymal carrier cells modulate tumor infiltrating immune cells and tumor microenvironment in mice with neuroblastoma. *Oncotarget.* 11, 347–61
- 41 Maris, J.M. et al. (2007) Neuroblastoma. *Lancet (London, England)* 369, 2106–20
- 42 Martín-Ruiz, A. et al. (2020) Benefits of exercise and immunotherapy in a murine model of human non-small-cell lung carcinoma. *Exerc. Immunol. Rev.* 26, 100–115
- 43 Fiuza-Luces, C. et al. (2013) Exercise benefits in chronic graft versus host disease: a murine model study. *Med. Sci. Sports Exerc.* 45, 1703–11
- 44 Fernández-de la Torre, M. et al. (2020) Exercise Training and Neurodegeneration in Mitochondrial Disorders: Insights From the Harlequin Mouse. *Front. Physiol.* 11, 594223
- 45 Fiuza-Luces, C. et al. (2019) Physical Exercise and Mitochondrial Disease: Insights From a Mouse Model. *Front. Neurol.* 10, 790
- 46 Welinder, C. and Ekblad, L. (2011) Coomassie staining as loading control in Western blot analysis. *J. Proteome Res.* 10, 1416–9
47. Salgado, C. Azevedo, C., Proença, H. and Vieira, S. (2016) Missing data. *Secondary Analysis of Electronic Health Records*. 1st ed. Springer, Cham, Switzerland, 143–162.
- 48 Fong, D.Y.T. et al. (2012) Physical activity for cancer survivors: meta-analysis of randomised controlled trials. *BMJ* 344, e70
- 49 McMillan, E.M. and Newhouse, I.J. (2011) Exercise is an effective treatment modality for reducing cancer-related fatigue and improving physical capacity in cancer patients and survivors: a meta-analysis. *Appl. Physiol. Nutr. Metab.* 36, 892–903
- 50 Elshahat, S. et al. (2021) Factors influencing physical activity participation among people living with or beyond cancer: a systematic scoping review. *Int. J. Behav. Nutr. Phys. Act.* 18, 50

- 51 Schmid, D. and Leitzmann, M.F. (2015) Cardiorespiratory fitness as predictor of cancer mortality: a systematic review and meta-analysis. *Ann. Oncol. Off. J. Eur. Soc. Med. Oncol.* 26, 272–8
- 52 Clifford, B. et al. (2021) The Effect of Resistance Training on Body Composition During and After Cancer Treatment: A Systematic Review and Meta-Analysis. *Sports Med.* 51, 2527–46
- 53 Strasser, B. et al. (2013) Impact of resistance training in cancer survivors: a meta-analysis. *Med. Sci. Sports Exerc.* 45, 2080–90
- 54 Kawakubo, N. et al. (2019) The Influence of Sarcopenia on High-Risk Neuroblastoma. *J. Surg. Res.* 236, 101–5
- 55 Walsh, N.P. et al. Position statement part one: Immune function and exercise. , *Exercise Immunology Review*, 17. (2011), 6–63
- 56 Kruijssen-Jaarsma, M. et al. (2013) Effects of exercise on immune function in patients with cancer: a systematic review. *Exerc. Immunol. Rev.* 19, 120–43
- 57 Llaverro, F. et al. (2021) Exercise training effects on natural killer cells: a preliminary proteomics and systems biology approach. *Exerc. Immunol. Rev.* 27, 125–41
- 58 MacDonald, G. et al. (2021) A pilot study of high-intensity interval training in older adults with treatment naïve chronic lymphocytic leukemia. *Sci. Rep.* 11, 3137
- 59 Toffoli, E.C. et al. (2021) Effects of physical exercise on natural killer cell activity during (neo)adjuvant chemotherapy: A randomized pilot study. *Physiol. Rep.* 9, e14919
- 60 Schenk, A. et al. (2022) Distinct distribution patterns of exercise-induced natural killer cell mobilization into the circulation and tumor tissue of patients with prostate cancer. *Am. J. Physiol. Cell Physiol.* 323, C879–84
- 61 Schauer, T. et al. (2022) The effects of acute exercise and inflammation on immune function in early-stage prostate cancer. *Brain Behav Immun Health* 25, 100508
- 62 Djurhuus, S.S. et al. (2022) Effects of acute exercise training on tumor outcomes in men with localized prostate cancer: A randomized controlled trial. *Physiol Rep* 10, e15408
- 63 Timmons, B.W. and Cieslak, T. (2008) Human natural killer cell subsets and acute exercise: a brief review. *Exerc. Immunol. Rev.* 14, 8–23
- 64 Djurhuus, S.S. et al. Exercise training to increase tumour natural killer-cell infiltration in men with localised prostate cancer: a randomised controlled trial. *BJU Int.* 131, 116–24
- 65 Valenzuela, P.L. et al. (2022) Exercise Training and Natural Killer Cells in Cancer Survivors: Current Evidence and Research Gaps Based on a Systematic Review and Meta-analysis. *Sport. Med.* - open 8, 36
- 66 Hagar, A. et al. (2019) Endurance training slows breast tumor growth in mice by suppressing Treg cells recruitment to tumors. *BMC Cancer* 9, 536
- 67 Gomes-Santos, I.L. et al. (2021) Exercise Training Improves Tumor Control by Increasing CD8+ T-cell Infiltration via CXCR3 Signaling and Sensitizes Breast Cancer to Immune Checkpoint Blockade. *Cancer Immunol. Res.* 9, 765–78
- 68 Rundqvist, H. et al. (2020) Cytotoxic T-cells mediate exercise-induced reductions in tumor growth. *Elife* 9, e59996
- 69 Kurz, E. et al. (2022) Exercise-induced engagement of the IL-15/IL-15R α axis promotes anti-tumor immunity in pancreatic cancer. *Cancer Cell* 40, 720-737.e5
- 70 Gupta, P. et al. (2022) Comparison of three exercise interventions with and without gemcitabine treatment on pancreatic tumor growth in mice: No impact on tumor infiltrating lymphocytes. *Front. Physiol.* 13, 1039988
- 71 Huang, M. and Weiss, W.A. (2013) Neuroblastoma and *MYCN*. *Cold Spring Harb. Perspect. Med.* 3, a014415
- 72 Layer, J.P. et al. (2017) Amplification of N-Myc is associated with a T-cell-poor microenvironment in metastatic neuroblastoma restraining interferon pathway activity and chemokine expression. *Oncoimmunology* 6, e1320626
- 73 Vanichapol, T., Chutipongtanate, S., Anurathapan, U. and Hongeng S. (2018) Immune Escape Mechanisms and Future Prospects for Immunotherapy in Neuroblastoma. *Biomed. Res. Int.* 2018, 1812535
- 74 Chen, D.S. and Mellman, I. (2017) Elements of cancer immunity and the cancer-immune set point. *Nature* 541, 321–30
- 75 Wienke, J. et al. (2021) The immune landscape of neuroblastoma: Challenges and opportunities for novel therapeutic strategies in pediatric oncology. *Eur. J. Cancer* 144, 123–50
- 76 Melaiu, O. et al. (2020) Cellular and gene signatures of tumor-infiltrating dendritic cells and natural-killer cells predict prognosis of neuroblastoma. *Nat. Commun.* 11, 5992
- 77 Redlinger, R.E. et al. (2004) Neuroblastoma and dendritic cell function. *Semin. Pediatr. Surg.* 13, 61–71
- 78 Shurin, G.V. et al. (2001) Neuroblastoma-derived gangliosides inhibit dendritic cell generation and function. *Cancer Res.* 61, 363–9
- 79 Yang, J. et al. (2022) A novel ganglioside-related risk signature can reveal the distinct immune landscape of neuroblastoma and predict the immunotherapeutic response. *Front. Immunol.* 13, 1061814
- 80 Walker, S.R., Redlinger, R.E. Jr. and Barksdale, E.M. Jr. (2005) Neuroblastoma-induced inhibition of dendritic cell IL-12 production via abrogation of CD40 expression. *J. Pediatr. Surg.* 40, 244–9
- 81 Harada, K. et al. (2019) Soluble factors derived from neuroblastoma cell lines suppress dendritic cell differentiation and activation. *Cancer Sci.* 110, 888–902
- 82 Zafari, R., Razi, S. and Rezaei, N. (2022) The role of dendritic cells in neuroblastoma: Implications for immunotherapy. *Immunobiology* 227, 152293.
- 83 Broz, M.L. et al. (2014) Dissecting the tumor myeloid compartment reveals rare activating antigen-presenting cells critical for T cell immunity. *Cancer Cell* 26, 638–52
- 84 Ruffell, B. et al. (2014) Macrophage IL-10 blocks CD8+ T cell-dependent responses to chemotherapy by suppressing IL-12 expression in intratumoral dendritic cells. *Cancer Cell* 26, 623–37
- 85 Cordeau, M., et al. (2016) Efficient Killing of High Risk Neuroblastoma Using Natural Killer Cells Activated by Plasmacytoid Dendritic Cells. *PLoS One.* 2016 11, e0164401
- 86 Belounis, A., et al. (2020) Patients' NK cell stimulation with activated plasmacytoid dendritic cells increases dinutuximab-induced neuroblastoma killing. *Cancer Immunol. Immunother.* 69, 1767–79
- 87 Zafari, R., Razi, S. and Rezaei, N. (2022) The role of dendritic cells in neuroblastoma: Implications for immunotherapy. *Immunobiology* 227, 152293.
- 88 Bianco, T.M. et al. (2017) The influence of physical activity in the anti-tumor immune response in experimental breast tumor. *Immunol. Lett.* 190, 148–58
- 89 Asgharzadeh, S. et al. (2012) Clinical significance of tumor-associated inflammatory cells in metastatic neuroblastoma. *J.*

- Clin. Oncol. 30, 3525–32
- 90 Mao, Y. et al. (2016) Targeting Suppressive Myeloid Cells Potentiates Checkpoint Inhibitors to Control Spontaneous Neuroblastoma. *Clin. Cancer Res.* 22, 3849–59
- 91 Lamkin, D.M. et al. (2021) Physical activity modulates mononuclear phagocytes in mammary tissue and inhibits tumor growth in mice. *Peer. J.* 9, e10725
- 92 Ge, Z., Wu, S., Qi, Z. and Ding, S. (2022) Exercise modulates polarization of TAMs and expression of related immune checkpoints in mice with lung cancer. *J Cancer* 13, 3297–307
- 93 Denton, N.L. et al. (2016) Tumor-Associated Macrophages in Oncolytic Virotherapy: Friend or Foe? *Biomedicines* 4, 1–12
- 94 Boada-Romero, E. et al. (2020) The clearance of dead cells by efferocytosis. *Nat. Rev. Mol. Cell Biol.* 21, 398–414
- 95 Pedersen, L. et al. (2016) Voluntary Running Suppresses Tumor Growth through Epinephrine- and IL-6-Dependent NK Cell Mobilization and Redistribution. *Cell Metab.* 23, 554–62
- 96 Wennerberg, E. et al. (2020) Exercise reduces immune suppression and breast cancer progression in a preclinical model. *Oncotarget* 11, 452–461
- 97 Garritson, J. et al. (2020) Physical activity delays accumulation of immunosuppressive myeloid-derived suppressor cells. *PLoS One* 15, e0234548
- 98 Schmidt, T. et al. (2018) Influence of physical activity on the immune system in breast cancer patients during chemotherapy. *J. Cancer Res. Clin. Oncol.* 144, 579–586
- 99 Niemi, G.M. et al. (2022) Salutary effects of moderate but not high intensity aerobic exercise training on the frequency of peripheral T-cells associated with immunosenescence in older women at high risk of breast cancer: a randomized controlled trial. *Immun. Ageing* 19, 17
- 100 Duggal, N.A. et al. (2018) Major features of immunosenescence, including reduced thymic output, are ameliorated by high levels of physical activity in adulthood. *Aging Cell* 17, 1–12
- 101 Rosa-Neto, J.C. et al. (2022) Immunometabolism-fit: How exercise and training can modify T cell and macrophage metabolism in health and disease. *Exerc. Immunol. Rev.* 28, 29–46
- 102 Betof, A.S. et al. (2015) Modulation of murine breast tumor vascularity, hypoxia and chemotherapeutic response by exercise. *J. Natl. Cancer Inst.* 107, 1–12
- 103 Jones, L.W. et al. (2010) Effect of aerobic exercise on tumor physiology in an animal model of human breast cancer. *J. Appl. Physiol.* 108, 343–8
- 104 Jones, L.W. et al. (2012) Exercise modulation of the host-tumor interaction in an orthotopic model of murine prostate cancer. *J. Appl. Physiol.* 113, 263–72
- 105 McCullough, D.J. et al. (2014) Modulation of blood flow, hypoxia, and vascular function in orthotopic prostate tumors during exercise. *J. Natl. Cancer Inst.* 106, dju036
- 106 McCullough, D.J. et al. (2013) Effects of exercise training on tumor hypoxia and vascular function in the rodent preclinical orthotopic prostate cancer model. *J. Appl. Physiol.* 115, 1846–54
- 107 Schadler, K.L. et al. (2016) Tumor vessel normalization after aerobic exercise enhances chemotherapeutic efficacy. *Oncotarget* 7, 65429–65440
- 108 Sturgeon, K. et al. (2014) Concomitant low-dose doxorubicin treatment and exercise. *Am. J. Physiol. Regul. Integr. Comp. Physiol.* 307, R685–92
- 109 Jones, L.W. and Dewhirst, M.W. (2014) Therapeutic properties of aerobic training after a cancer diagnosis: more than a one-trick pony? *J. Natl. Cancer Inst.* 106, dju042
- 110 Chow, L.S. et al. (2022) Exerkines in health, resilience and disease. *Nat. Rev. Endocrinol.* 18, 273–289
- 111 Wang, L. et al. (2022) MCP-1 targeting: Shutting off an engine for tumor development. *Oncol. Lett.* 23, 26
- 112 McFarland, D.C. et al. (2022) Cancer-related inflammation and depressive symptoms: Systematic review and meta-analysis. *Cancer DOI: 10.1002/cncr.34193*
- 113 Orange, S.T. et al. (2020) The serological responses to acute exercise in humans reduce cancer cell growth in vitro: A systematic review and meta-analysis. *Physiol. Rep.* 8, e14635
- 114 Kim, J.-S. et al. (2021) Exercise-induced myokines and their effect on prostate cancer. *Nat. Rev. Urol.* 18, 519–542
- 115 Kim, J.-S. et al. (2022) Myokine Expression and Tumor-Suppressive Effect of Serum after 12 wk of Exercise in Prostate Cancer Patients on ADT. *Med. Sci. Sports Exerc.* 54, 197–205
- 116 Kim, J.-S. et al. (2022) Exercise in advanced prostate cancer elevates myokine levels and suppresses in-vitro cell growth. *Prostate Cancer Prostatic Dis.* 25, 86–92
- 117 Rundqvist, H. et al. (2013) Effect of acute exercise on prostate cancer cell growth. *PLoS One* 8, e67579
- 118 Dethlefsen, C. et al. (2016) Exercise regulates breast cancer cell viability: systemic training adaptations versus acute exercise responses. *Breast Cancer Res. Treat.* 159, 469–79
- 119 Devin, J.L. et al. (2019) Acute high intensity interval exercise reduces colon cancer cell growth. *J. Physiol.* 597, 2177–2184
- 120 Rincón-Castaneda, C. et al. (2020) Physical exercise effects on metastasis: a systematic review and meta-analysis in animal cancer models. *Cancer Metastasis Rev.* 39, 91–114
- 121 Woods, J.A. et al. (1994) Effects of exercise on the immune response to cancer. *Med. Sci. Sports Exerc.* 26, 1109–15
- 122 Zheng, X. et al. (2008) Inhibitory effect of voluntary running wheel exercise on the growth of human pancreatic Panc-1 and prostate PC-3 xenograft tumors in immunodeficient mice. *Oncol. Rep.* 19, 1583–8
- 123 Esser, K.A. et al. (2009) Physical activity reduces prostate carcinogenesis in a transgenic model. *Prostate* 69, 1372–7
- 124 Zielinski, M.R. et al. (2004) Exercise delays allogeneic tumor growth and reduces intratumoral inflammation and vascularization. *J. Appl. Physiol.* 96, 2249–56
- 125 Buss, L.A., et al. (2021) Effects of exercise and anti-PD-1 on the tumour microenvironment. *Immunol Lett* 239, 60–71.
- 126 Li, J. et al. (2019) Prognostic value of TGF- β in lung cancer: systematic review and meta-analysis. *BMC Cancer* 19, 691
- 127 Ungefroren, H. (2021) Autocrine TGF- β in Cancer: Review of the Literature and Caveats in Experimental Analysis. *Int. J. Mol. Sci.* 22, 977
- 128 Chen, Y. et al. (2020). Transforming growth factor β signaling pathway: A promising therapeutic target for cancer. *J. Cell Physiol.* 235, 1903–14
- 129 Cardoso, C.C. et al. (2010) Optimizing orthotopic cell transplantation in the mouse adrenal gland. *Cell Transplant.* 19, 565–72
- 130 Ornell, K.J. and Coburn, J.M. (2019) Developing preclinical models of neuroblastoma: driving therapeutic testing. *BMC Biomed. Eng.* 1, 33

Supplemental file 1. Primary and secondary antibodies used in this study for western blot analyses of markers of muscle molecular adaptations to training at the skeletal muscle level.

	Antibody	Dilution	Provider	Reference
Primary antibodies	Catalase	1:1000	Sigma	C0979
	Citrate synthase	1:1000	Abcam	ab96600
	Gluthathione reductase	1:1000	Abcam	ab16801
	mtSOD	1:1000	MERCK Millipore	06-984
	OXPPOS rodent WB antibody cocktail*	1:250	Abcam	ab110413
	P70S6K	1:1000	Cell Signaling	9202
	pP70S6K (Thr389)	1:1000	Cell Signaling	9205
Secondary antibodies	Goat Anti-Mouse	1:3000	Abcam	ab205719
	Goat Anti-Rabbit	1:3000	Abcam	ab205718

Abbreviations: mtSOD, mitochondrial superoxide dismutase; OXPPOS, oxidative phosphorylation system; P70S6K, ribosomal protein p70 S6 kinase; pP70S6K, activated/phosphorylated P70S6K; WB, western blotting. Symbol: *This cocktail allows to determine all five mitochondrial respiratory complexes (CI to CV) simultaneously.

Supplemental file 2. Primary and secondary antibodies used for immunohistochemical analyses in tumors.

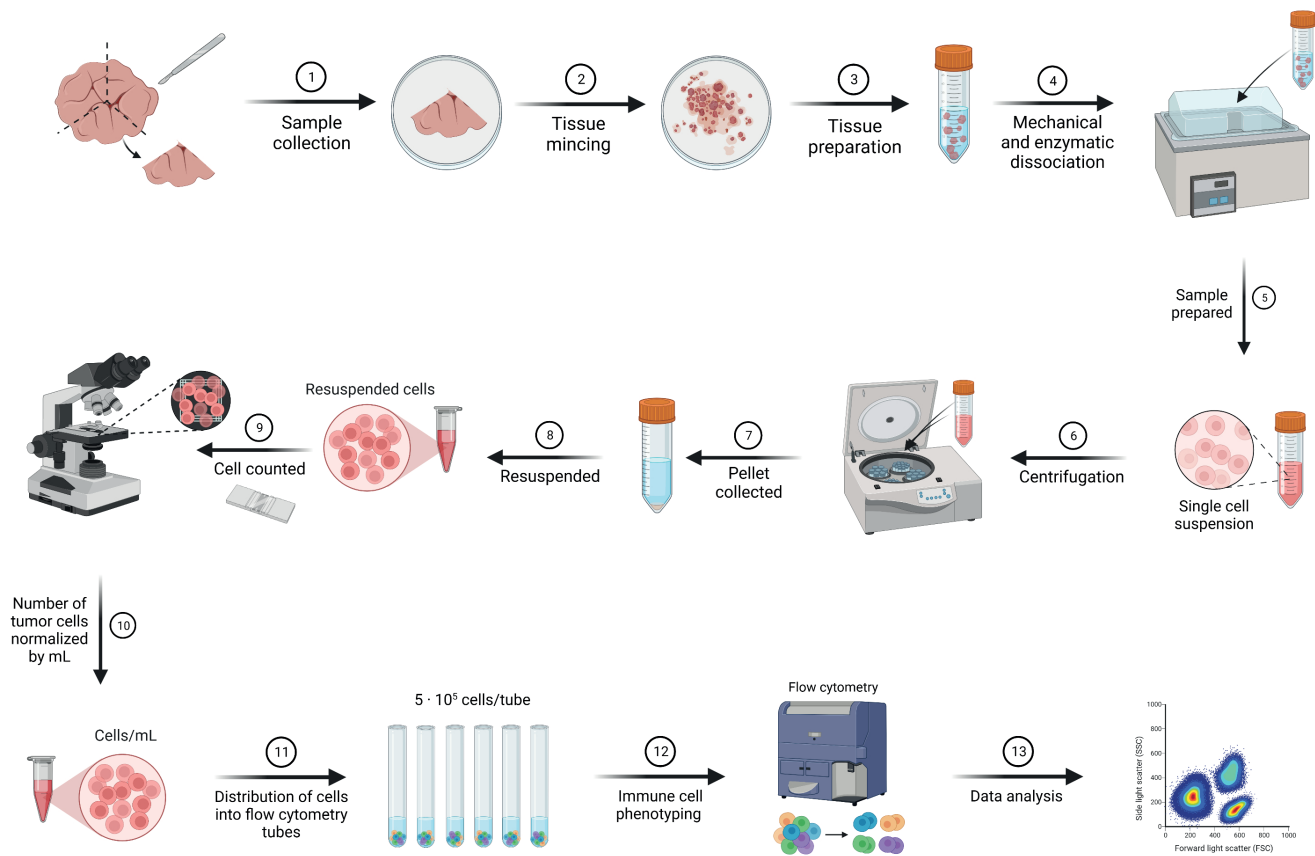
Antibody	Dilution	Provider	Reference
Cleaved Caspase-3 (Asp175) (5A1E)	1:400	Cell Signaling	9664
Histone H3 (D1H2)	1:100	Cell Signaling	4499
Ki-67 (D3B5)	1:1000	Cell Signaling	12202
VEGFR2 (55B11)	1:500	Cell Signaling	2479
Von Willebrand Factor (Factor VIII-related antigen)	1:100	Agilent	GA527

Abbreviation: VEGFR2, vascular endothelial growth factor receptor 2.

Supplemental file 3. Flow cytometry antibodies.

Tube	Antibody	Fluorophore	Provider	Reference
1	CD11b	APC	BioLegend	101212
	CD11c	APC/Cyanine7	BioLegend	117324
	CD45	Brilliant Violet 510™	BioLegend	103138
	CD45R/B220	FITC	BioLegend	103206
	CD3ε	PE	BioLegend	100308
	NK-1.1	PE/Cy7	BioLegend	108714
	7AAD Viability Staining	PERCP/CY7	BioLegend	420404
2	CD8a	APC	BioLegend	100712
	Ly-6A/E (Sca-1)	APC/Cyanine7	BioLegend	108125
	CD62L	Brilliant Violet 510™	BioLegend	104441
	CD4	Pacific Blue™	BioLegend	100531
	CD44	FITC	BioLegend	103022
	CD122 (IL-2Rβ)	PE	BioLegend	123209
	CD95	PE/Cy7	BD	557653
	7AAD Viability Staining	PERCP/CY7	BioLegend	420404
3	CD8a	APC	BioLegend	100712
	CD25	APC/Cyanine7	BioLegend	102026
	CD45	Brilliant Violet 510™	BioLegend	103138
	CD134 / OX40	FITC	Fisher	MA5-17917
	CD4	Pacific Blue™	BioLegend	100531
	CD3ε	PE	BioLegend	100308
	CD152 (CTLA-4)	PE/Cy7	BioLegend	106313
	7AAD Viability Staining	PERCP/CY7	BioLegend	420404
4	CD137 (4-1BB)	FITC	BioLegend	558975
	CD223 (LAG-3)	PE	BioLegend	125207
	CD366 (Tim-3)	PE/Cy7	BioLegend	119715
	CD279 (PD-1)	APC/Cy7	BioLegend	135223
	7AAD Viability Staining	PERCP/CY7	BioLegend	420404
5	CD11b	APC	BioLegend	101212
	Ly-6G	APC/Cy7	BioLegend	127624
	CD45	Brilliant Violet 510™	BioLegend	103138
	CD206 (MMR)	FITC	BioLegend	141704
	Ly-6C	Pacific Blue™	BioLegend	128013
	7AAD Viability Staining	PERCP/CY7	BioLegend	420404
6	CD11b	APC	BioLegend	101212
	CD11c	APC/Cyanine7	BioLegend	117324
	CD45	Brilliant Violet 510™	BioLegend	103138
	CD103	FITC	BioLegend	121419
	CD123	PE	BioLegend	106005
	7AAD Viability Staining	PERCP/CY7	BioLegend	420404

Supplemental file 4. Procedures used from tumor sample collection to final immune cell phenotyping with flow cytometry.



Supplemental file 5. Immunophenotype determination in the tumors with flow cytometry. **A.** Strategy to analyze flow cytometry data. **B.** Flow cytometry plots from an example of ‘hot-like’ tumor. When the viability of CD45+ (total leukocytes) infiltrates in the tumor using 7AAD labelling was analyzed, it was found that 38.9% of these cells were alive. Thus, the main immune subsets were subsequently detectable. **C.** Flow cytometry plots from an example of ‘cold-like’ tumor. When the viability of CD45+ (total leukocytes) infiltrates in the tumor using 7AAD labelling was analyzed, it was found that 1.2% of these cells were alive. This value represented a 0.3% of the total ‘events’ analyzed. Thus, the main immune subsets were subsequently undetectable.

